FI SEVIER

Contents lists available at ScienceDirect

### Journal of Archaeological Science: Reports

journal homepage: www.elsevier.com/locate/jasrep



# Late Holocene forager-fisher and pastoralist interactions along the Lake Victoria shores, Kenya: Perspectives from portable XRF of obsidian artifacts



Ellery Frahm a,b,c,\*, Steven T. Goldstein d, Christian A. Tryon b

- a Yale Center for the Study of Ancient Pyrotechnology, Department of Anthropology, Yale University, 10 Sachem Street, New Haven, CT 06511, United States
- <sup>b</sup> Department of Anthropology, Harvard University, Peabody Museum, 11 Divinity Avenue, Cambridge, MA 02138, United States
- <sup>c</sup> Department of Anthropology, University of Minnesota, Humphrey Center #395, 301 19th Avenue S, Minneapolis, MN 55455, United States
- d Department of Anthropology, Washington University in St. Louis, CB 1114 1 Brookings Drive, St. Louis, MO 63130, United States

#### ARTICLE INFO

## Article history: Received 2 June 2016 Received in revised form 15 December 2016 Accepted 7 January 2017 Available online 21 January 2017

Keywords:
Later Stone Age
Eastern Africa
Lake Victoria
Forager-pastoralist interactions
Obsidian artifact sourcing
Portable XRF (pXRF)
Analytical cross-calibration

#### ABSTRACT

The East African Rift system created one of the world's most obsidian-rich landscapes, where this volcanic glass has been used to make tools for nearly two million years. In Kenya alone, there are >80 chemically distinct obsidians along a 800-km north-south transect. Recently Brown et al. (2013) published their Kenyan obsidian database assembled since the 1980s. Specifically, they report elemental data measured by EMPA, ICP-MS, and WDXRF, providing a rich basis for future sourcing studies. Here we report our use of portable XRF (pXRF), calibrated specifically and directly to the database in Brown et al. (2013), to examine interactions between Later Stone Age forager-fishers and pastoralists near Lake Victoria. Regarding our calibration to the WDXRF and EMPA datasets of Brown et al. (2013), the elements of interest have very high correlations ( $R^2 = 0.96-0.99$ ) to our pXRF values, which show, on average, only a 2-5% relative difference from the published values. Use of pXRF data specifically calibrated to the datasets from Brown et al. (2013) greatly expands the impact of their work over three decades to catalog and characterize a multitude of Kenyan obsidians. Our focus here is investigating social contacts and exchange between late Holocene populations that included Kansyore forager-fishers and Elmenteitan pastoralists. Similarities and differences in their obsidian access provide new insights into long-term interactions between foragers and food producers in eastern Africa. We report new sourcing results for obsidian artifacts from six late Holocene rock shelters along the Winam Gulf of Lake Victoria. The patterns in obsidian access are consistent with changing interaction spheres that are relevant to understanding forager-fisher social identities and subsistence strategies during periods of economic and demographic change.

© 2017 Elsevier Ltd. All rights reserved.

#### 1. Introduction

Volcanism of the East African Rift, where the African tectonic plate is splitting in two, created one of the world's most obsidian-rich land-scapes, where this volcanic glass has been used, perhaps continuously, to make tools for almost two million years (Leakey, 1971; Clark and Kurashina, 1981; Brandt et al., 1996; Brandt and Weedman, 1997; Piperno et al., 2009). Many dozens of obsidian sources lie between Eritrea in the north and Tanzania in the south. There are, by some tallies (Brown et al., 2013), >80 chemically distinct obsidians in Kenya alone. It is unsurprising, therefore, that archaeologists have long been interested to trace the distribution of obsidians across the region (e.g., Merrick

 $\textit{E-mail addresses:} \ ellery frahm@gmail.com, frah0010@umn.edu \ (E.\ Frahm).$ 

and Brown, 1984a, b; Merrick et al., 1988, 1994; Negash and Shackley, 2006; Coleman et al., 2008; Nash et al., 2011; Ndiema et al., 2011; Ambrose, 2012). Before the successes of chemical obsidian sourcing (Cann and Renfrew, 1964), researchers sought to match obsidian artifacts to these sources using density, refractive index, and similar physical properties (Lucas, 1942, 1947; Leakey, 1945). Surveys of the southern Kenya Rift (Bower et al., 1977) revealed a greater number of obsidians than anticipated, complicating the potential for sourcing research. To conduct obsidian sourcing in Kenya, for example, one must first sample the multitude of obsidian sources that occur along a 800-km stretch between Lake Turkana on the Ethiopian border and Lake Natron on the Tanzanian border (Fig. 1). Alternatively, one could utilize a coherent, published database of Kenyan obsidians – that is, if the measurements of obsidian artifacts are sufficiently compatible with an existing source database.

Recently Brown et al. (2013) published their full Kenyan obsidian source database, assembled since the 1980s (Merrick and Brown,

<sup>\*</sup> Corresponding author at: Yale Center for the Study of Ancient Pyrotechnology, Department of Anthropology, Yale University, 10 Sachem Street, New Haven, CT 06511, United States.

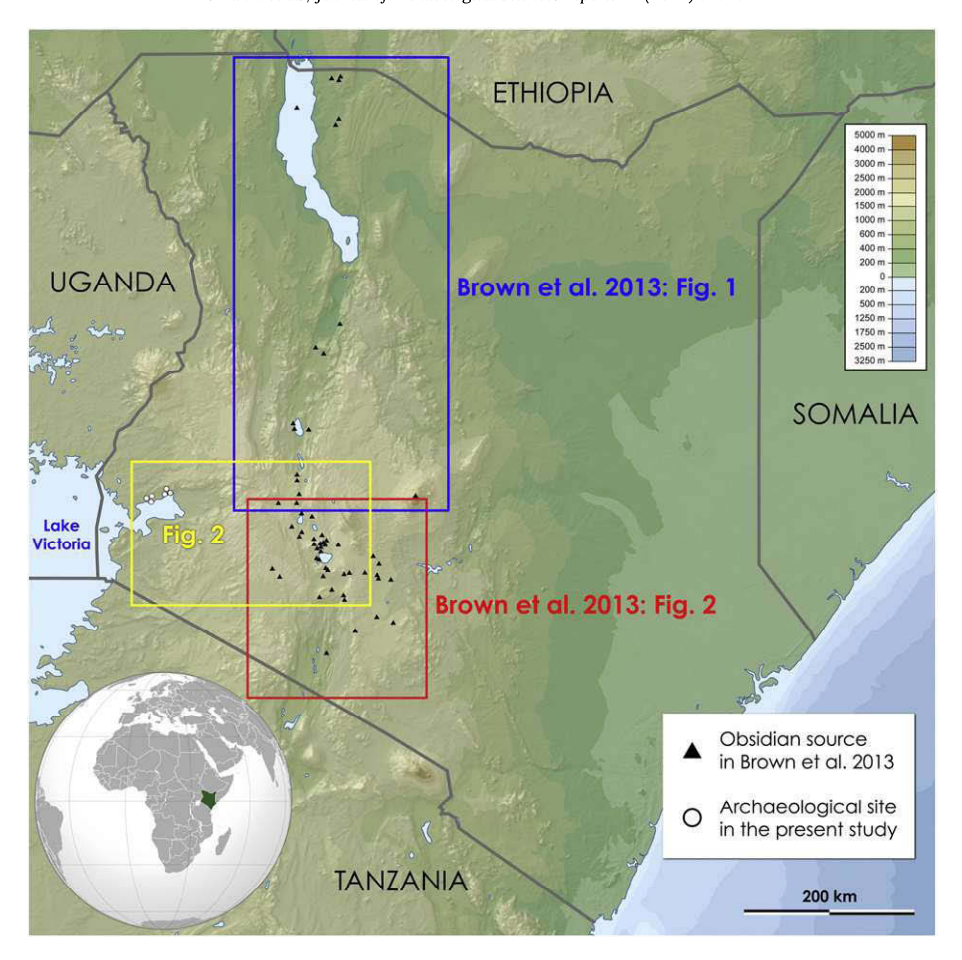


Fig. 1. Locations of Kenyan obsidian sources (black triangles) published by Brown et al. (2013) and the six Late/Terminal Kansyore rock shelters excavated by Gabel (1969) along the Lake Victoria shore (white circles). Insets correspond to figures in Brown et al. (2013) (red and blue) and to Fig. 2 here (yellow). Background map source: NASA Shuttle Radar Topography Mission (SRTM3).

1984a). Specifically, they report elemental data for 194 geological obsidian specimens from 90 localities across Kenya. From these specimens, small subsamples were prepared for (i.e., cut, mounted, ground, and polished) and measured by electron microprobe analysis (EMPA), specifically a CAMECA SX-50, using conditions found in Nash (1992). The original EMPA measurements in Merrick and Brown (1984a) were acquired using an ARL-EMX, an instrument from the 1960s that output data onto punch cards. Therefore, their new EMPA data represent a considerable improvement. The same subsamples were measured using inductively coupled plasma mass spectrometry (ICP-MS) with laser ablation, specifically an Agilent 7500ce quadrupole mass spectrometer, using conditions reported in Eggins (2003). Other subsamples were prepared for (crushed and finely powdered) and measured by wavelength-dispersive X-ray fluorescence (WDXRF), specifically a Fisons (now Thermo Scientific) 6400 instrument, using conditions reported in Brown et al. (2006). Consequently, their published database includes EMPA, WDXRF, and ICP-MS data for the same suite of obsidian specimens, providing a rich basis on which other researchers can build archaeological studies involving artifact sourcing.

The last few years have seen the rise and proliferation of portable X-ray fluorescence (pXRF) in obsidian sourcing. Such instruments offer archaeologists a number of advantages over analytical techniques traditionally used for sourcing. First, pXRF is a non-destructive technique, meaning that the artifacts do not need to be polished, powdered, or disposed as radioactive waste. Second, it is rapid, frequently requiring only a minute or two to measure dozens of elements. Third, it can be conducted at a museum, in a field house, or even at an archaeological site. Thus, artifacts can be sourced without concern for the practical, legal, or ethical limitations associated with distant instruments or destructive techniques.

The adoption of pXRF, however, is not without controversy. One concern expressed in the literature (e.g., Shackley, 2012b; Speakman and Shackley, 2013) and at conferences (e.g., Brandt et al., 2013) is that pXRF datasets are not - due to technical limitations or user inexperience – compatible with data from other analytical techniques. However, this is not an issue particular to pXRF. Instead, it is unwise to uncritically integrate datasets from any combination of measuring devices, be they spectrometers or bathroom scales. Recent pXRF instruments indeed have the technical capacity for high accuracy and reproducibility, which are attainable using suitable methods (Frahm, 2014a). Another concern is that pXRF lacks the sensitivity needed to distinguish chemically similar obsidian sources in complex regions (e.g., Shackley, 2011a). Yet pXRF can make subtle source distinctions that once required neutron activation analysis (NAA; Frahm and Feinberg, 2015), exhibiting greater analytical sensitivity than conventional labbased XRF instruments only a decade ago.

Here we report our use of pXRF, specifically calibrated and compared to the datasets in Brown et al. (2013), to study interactions between Later Stone Age (LSA) foragers and food producers near the eastern shore of Lake Victoria. Regarding our direct calibration to the WDXRF and EMPA datasets from Brown et al. (2013) using matched specimens from their reference collection, the elements of interest for assigning obsidian artifacts to their geological sources (e.g., Zr, Nb, Rb) exhibit very high correlations ( $R^2=0.96-0.99$ ) to our pXRF measurements. Once calibrated to the Brown et al. (2013) data, our pXRF measurements exhibit, on average, only a 2–5% relative difference, akin to compatible datasets in other studies using lab-based instruments. In addition, when our new pXRF measurements of geological specimens are plotted with published data, they directly overlap, further

demonstrating that the published values and our pXRF values are directly compatible and suitable for such a study. As with any sourcing work, the strength of the artifact attributions is predicated on the comprehensiveness of the source database. Here we use the database of Brown et al. (2013), but such work is not complete. In Kenya and surrounding regions, our knowledge of obsidian sources and their utilization in the past continues to improve due to ongoing endeavors (e.g., Coleman et al., 2008, 2009; Brandt and Johnson, 2011; Ambrose, 2012; Ambrose et al., 2012a, b; Ferguson, 2012; Slater et al., 2012; Brandt et al., 2013, 2014; Brandt, 2015; Slater and Ambrose, 2015).

Our results suggest that late Holocene fisher-foragers in the Lake Victoria region maintained sophisticated social contacts with mobile herders and sedentary farmers across several centuries. There are outstanding questions concerning the nature of forager-food producer relationships in this region and how such interactions may have been integrated into the long-term resilience of these groups. Addressing such questions is considered an essential – but elusive – step in understanding the spread of African mobile herding, the persistence of forager lifeways into the present, and the sustainability of these lifeways in unpredictable environments with dispersed resources (e.g., Dale and Ashley, 2010; Gifford-Gonzalez, 2016; Marshall et al., 2011; Lane, 2004; Prendergast and Lane, 2010).

Reconstructing the movement and exchange of obsidian artifacts is a promising line of investigation to elucidate the interaction spheres of Holocene foragers, which, in the Lake Victoria region, included groups defined by the use of "Kansyore" ceramics (Dale and Ashley, 2010). Lacking sources of high-quality obsidian in the immediate vicinity, fisher-foragers in the Lake Victoria region relied primarily on local quartz sources. Merrick and Brown (1984b) report that, in "Early Kansyore" (~ 8000-7000 cal BP) contexts, obsidian is sparse and derives from a variety of sources near Lake Naivasha, including Mt. Eburru, ~200 km to the east (Fig. 2). This lies well beyond the known boundaries of Kansyore material culture. Therefore, small-scale acquisition of distant obsidians likely reflects varied forms of exchange among the diverse foragers occupying the Central Rift Valley and the Loita-Mara plains (Ambrose, 1998). When pastoralists linked to "Elmenteitan" material culture become archaeologically visible near Lake Victoria in the late Holocene, obsidian is more abundant in Kansyore assemblages and originates primarily from Mt. Eburru (Merrick and Brown, 1984a, b). Obsidian in Kansyore assemblages, we propose, reflects changes through time in patterns of cultural interaction and exchange. These patterns are relevant for investigating how Kansyore (and other) forager-fishers manipulated their social identities and economic strategies during known periods of demographic and climatic change.

#### 2. Archaeological background

Increased monsoonal rainfall regimes fed an expansive system of lakes and rivers in some portions of Africa during the African Humid Phase after ~8000 BP, encouraging the development of complex fisher-forager traditions (e.g., Kuper and Kröpelin, 2006; Kusimba, 2013; Stojanowski et al., 2014). The nature of the archaeological and behavioral variability among late Holocene foragers in eastern Africa remains poorly understood (Wilshaw, 2016). The Kansyore tradition, one of the better-described archaeological complexes, is identified on the basis of its distinctively decorated ceramics (Dale and Ashley, 2010). Kansyore deposits are most abundant near Lake Victoria, where they occur at openair riverine sites, lakeshore shell middens, and rock shelters. Kansyoreproducing forager-fishers used a quartz-based LSA lithic industry and exploited a broad range of terrestrial and aquatic faunas (e.g., Dale et al., 2004; Prendergast, 2010; Seitsonen, 2010). Their economies were perhaps based on "moderate return" strategies that might have resulted from low residential mobility and a focus on seasonally variable subsistence practices, such as fishing, shellfish acquisition, wild game hunting, and plant and honey collection. Available chronological evidence suggests the existence of "Early" (~8000-7000 BP) and "Late/Terminal" (~3000-1500 BP) phases of the Kansyore tradition, but there is still a notable chronological gap that requires further investigation (Dale and Ashley, 2010; Prendergast et al., 2014). Obsidian source data from Early Kansyore strata at White Rock Point and Luanda (Robertshaw et al., 1983; Merrick and Brown, 1984b) indicate that obsidian is sparse (1.3-7.5% of the lithic assemblages), with 25% of the obsidian originating from Mt. Eburru and the remainder from other sources located near Lake Naivasha. These and other data (Faith et al., 2015) attest to well-established late Pleistocene-Holocene systems of obsidian acquisition in the Lake Victoria region well before the local introduction of pastoralist economies.

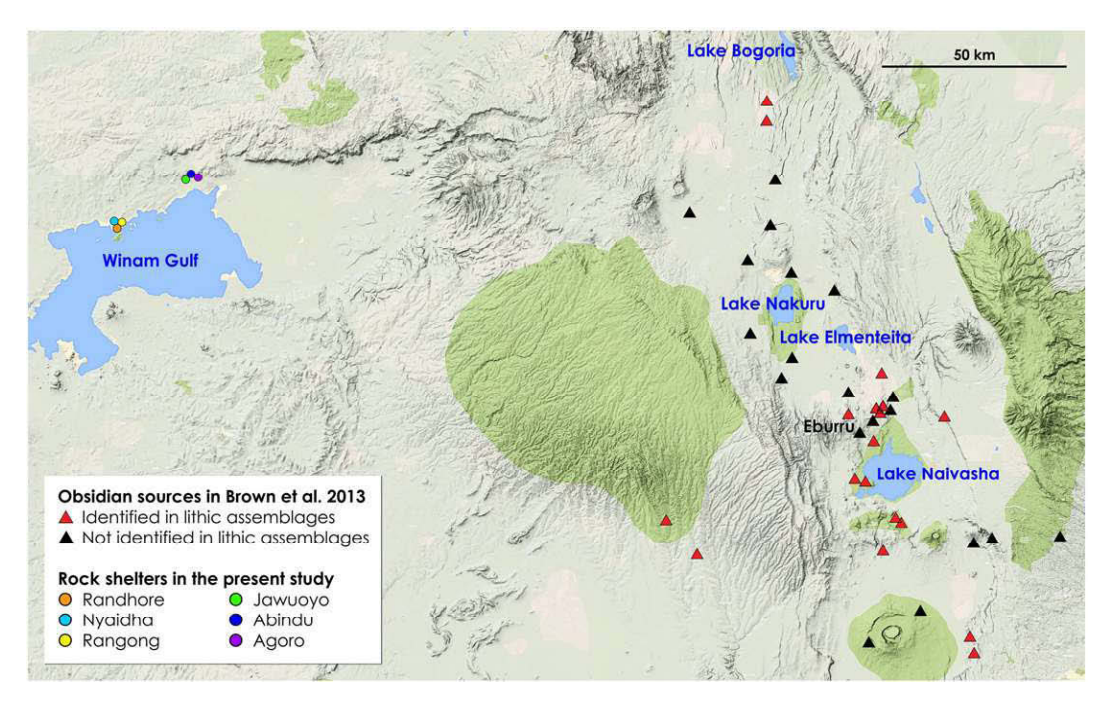


Fig. 2. Locations of Kenyan obsidian sources (triangles) in the Naivasha-Nakuru region published by Brown et al. (2013) and the six Late/Terminal Kansyore rock shelters in this study (circles). Obsidians that Brown et al. (2013) reported in archaeological assemblages are denoted by red triangles, while obsidians not identified in assemblages are denoted by black triangles. Background map source: Google Maps.

Table 1

In a "round robin" test conducted by Glascock (1999), eight labs, all experienced in obsidian sourcing, provided ten datasets for two geological specimens: one from Sierra de Pachuca and Frahm and Feinberg (2015) for Little Glass Buttes. The mean element concentrations across all labs are shown in the first column, and for each dataset, percent relative difference is calculated relative to the mean values, which can be considered as the best available "true" values (i.e., the values against which accuracy could be judged). The pXRF data in Frahm and Feinberg (2015) for Little Glass Buttes yielded some of the most accurate values (relative difference: 7% mean, 6% trimmed mean), demonstrating that portable instruments can be highly accurate.

	Sie	rra de Pa	achuca,	Sierra de Pachuca, Hidalgo, Mexico	Mexico																			
	ΙĞ	Glascock, 2011		Glascock, 1999	1999																			
Z	Mean Mt	MURR		MURR		CNRS Orléans	léans			Rio		CNRS Grenoble	enoble			ANSTO		Rome		Ashe,	Ashe Analytics		NW Obsidian	Mean
Λ		EDXRF %	%Diff I	NAA	%Diff	NAA	%Diff	LA-ICP-MS	%Diff	AES/MS	%Diff	. AES/MS	%Diff	PIXE	%Diff	F PIXE/PIGME	E %Diff	f WDXRF	: %Diff	f EDXRF	F %Diff	f EDXRF	F %Diff	
	18			30	51	21	17	6	65											20	0 12	2 14	1 23	
	1052					1160	10	2362	77				33	269										35
		15,900		15,800	9	17,200	3	16,600		16,	_	16,200		1	7 (	18,100	8 (	18	12	Ξ		_		
	1064	797	59	1149	8	066	7	1048																
QN	94	84	11			91	က	116						97						3 91	1 3	3 99	9 5	
Rb	202	189	7	192	2	219	∞	203																
Sr	4	10	88					2								3	3 25							
ц	1120	945	17			1300	15	1190		_		1049										114		
Zn	224	207	8	191	16	240	7	210						221	_			,-		224				
Zr	985	957	c	888	10	1020	m	1058				1005						1055			1 1			
Mean:			21		16		∞		25		23		16		8		14		13	3	11	_	6	
Trimme	Trimmed mean:		13		10		7		22		20		11		5		15		11	_	7	+	7	
	Litt	tle Glass	Buttes,	Little Glass Buttes, Oregon, United States	Inited S	tates																		
	Frahm Feinbo 2015	Frahm and Feinberg, 2015	<u>ن</u> ا	Glascock, 1999	666																			
4	Mean Mir	Minnesota	ı ∑ 	MURR	ן 	CNRS Orléans	ıns			Rio		CNRS Grenoble	oble			ANSTO		Rome		Ashe A	Ashe Analytics	NW OE	NW Obsidian	Mean
>	Value pXI	pXRF %Diff		NAA %D	%Diff N	NAA %D	%Diff LA-	LA-ICP-MS %	%Diff	AES/MS	%Diff	AES/MS	%Diff	PIXE	%Diff	PIXE/PIGME	%Diff	WDXRF	%Diff	EDXRF	%Diff	EDXRF	%Diff	%Diff
	1232 126	1265		1270	3 1!	1550	23	1080	13	843	37	1237	0							1270	3	1338	8	111
		78			5,		2	6813	13	5432	10	6219	4	2265	7	6230	4	5933	-					
	Ŋ	39		6200	5 65		0	6840	2	6100	9	6500	0	0209	7	7020	∞	7900	20	5730				
Mn	323 33	337		327			8	569	18	303	9	333	3	291	10	357	10	387	18	298				
S I		∞ ;	<sub>د</sub>			12	37	6	6	∞ ¦	m ·	∞ ;	co ·					9	32	7	16	∞	· .	13
Rb		94	9	95	4		10	97	7	92	4	94	9	105	9	109	6	97	7	96				
Sr	73	78	7	78				52	33	99	10	87	18	73	0	81	11	71	co	69				
F			17				2	595	10	009	6	527	22	788	18	691	2	629	<del></del>					
Zu	38				21	06	81	27	34	53	27			27	34	36	9			24	•			
Zr			18 1	118	15	66	m	83	70	106	4	106	4	105	3	107	2	105	n	96	9			
Mean:			7		∞		19		16		12		7		11		7		10		12		9	
Trimmed mean	1 теап:		9		7		13		15		10		2		6		7		∞		6		2	

In the Lake Victoria region south of the Winam Gulf (Figs. 1 and 2), archaeological deposits containing Kansyore ceramics are overlain by assemblages produced by stone-tool-using mobile pastoralists associated with the Elmenteitan tradition (after ~2000 cal. BP) and, subsequently, iron-using farmers with Urewe ceramics (by ~1200 cal. BP). North of the Winam Gulf, Kansyore strata are directly overlain directly by those containing Urewe ceramics at multiple localities (Lane, 2004). There is evidence (albeit from potentially mixed contexts) of domesticated livestock entering Late/Terminal Kansyore economies (Gabel, 1969; Karega-Műnene, 2002; Lane et al., 2007; Prendergast, 2010), and environmental data (Chritz et al., 2015) establish the suitability of the eastern margins of Lake Victoria for livestock during the late Holocene. These occasional traces of domestic fauna (cattle, sheep, goats) at Late/Terminal Kansyore sites have been interpreted as the outcome of limited contact with immigrating Elmenteitan pastoralist groups, but whether the traces reflect the exchange of individual animals with pastoralists, raiding of pastoralist livestock, or partial integration of herding into a foraging economy remains unclear (Karega-Mũnene, 2002; Lane et al., 2007; Prendergast, 2010).

Elmenteitan sites are identified by their uniform ceramic style and features of lithic technology. The latter includes small (~15-20 mm) microliths and large (~5-10 cm), heavily used blades that were produced by the punch technique and often segmented (Ambrose, 1984). Economies in Elmenteitan sites of the Loita-Mara region (e.g., Ngamuriak and Sambo Ngige) indicate a nearly exclusive reliance on domesticated cattle, sheep, and goat, whereas fish (and wild game) were also exploited at Gogo Falls, closer to lake Victoria (Marshall and Stewart, 1994; Robertshaw, 1988, 1991). Unlike Kansyore sites, where local stone materials predominate, Elmenteitan lithic assemblages are dominated by obsidian, regardless of their distance to the nearest source. Obsidian constitutes 71.4-98.3% of Elmenteitan lithic assemblages from Gogo Falls (~230 km linearly from the Lake Naivasha sources), Sambo Ngige (~170 km), and Ngamuriak (~100 km; Robertshaw, 1988, 1991), and it occurs with similar abundance at other sites (Olopilukunia, ~120 km, Siiriäinen, 1990; Wadh Lang'o, ~170 km, Lane et al., 2007). There is a consensus that the Elmenteitan pattern of obsidian access reflects some variety of regional exchange or distribution network (Ambrose, 2001; Gifford-Gonzalez, 1998; Goldstein, 2014; Robertshaw, 1988). Strikingly, Elmenteitan obsidian artifacts are largely (67%) from Mt. Eburru (Merrick and Brown, 1984a, 1984b; Merrick et al., 1988).

The Mt. Eburru source was used extensively despite the presence of closer sources west of Lake Naivasha (~10–20 km away). Elmenteitan groups did not exploit the nearest sources of similarly high-quality raw material as might be predicted by least-cost principles. Other obsidian sources, particularly those west of Lake Naivasha, seem to have been favored by contemporary but archaeologically distinct populations attributed to the Savanna Pastoral Neolithic (SPN), sites of which are not found on the margins of Lake Victoria. These patterns imply that, among Late Holocene pastoralist groups, there was a form of culturally mediated restrictions to obsidian sources (Ambrose, 2012).

Early Kansyore foragers during the early-mid Holocene apparently used obsidian sparingly, and when they did, it originated from various sources. In contrast, Elmenteitan pastoralists used obsidian in abundance and primarily from a single source (Mt. Eburru). The extent to which obsidian acquisition and use changed during the later Holocene at Late/Terminal Kansyore and other sites provides insights about the nature of differentiation and interaction among populations who made these archaeological complexes. While insufficient in isolation, obsidian sourcing data can complement insights based on stratigraphic, chronological, ceramic, lithic, and faunal datasets. We begin these comparisons by presenting our new chemical source attributions, based on pXRF analyses, for a collection of 78 obsidian artifacts from six late Holocene fisher-forager assemblages, which likely reflect Late/Terminal Kansyore material culture, from the northeastern shores of Lake Victoria.

#### 3. Terminology notes: "sources" and "pXRF"

It is worth briefly addressing how an individual obsidian "source" is conceptualized in this paper. The literature includes a plethora of terms to define and distinguish obsidian sources and hierarchies among them (see discussions in Green, 1998; Hughes, 1998; Frahm, 2014b). There are two principal ways in which an obsidian "source" is conceptualized and defined: geographically (i.e., a location on the land) and chemically (i.e., a cluster in chemical data). The difference is whether a source is described by a dot on a map or by a cluster in a plot of chemical data. Ideally, of course, one dot is the same as one cluster, but it is rarely so simple as each outcrop exhibiting a unique chemical composition. There are advocates for both geographical (Harbottle, 1982; Neff, 1998) and chemical (Hughes, 1998; Wilson and Pollard, 2001) definitions of a source, and both have appropriate applications.

Brown et al. (2013) favor the chemical definition of an obsidian source, but they also report named geographical locales, reflecting how obsidian is collected on the landscape. If different locales have obsidian with the same elemental composition ("fingerprint"), Brown et al. (2013) group them together into one chemical source. For example, twelve obsidian specimens from seven locations on Mt. Eburru comprise one source ("Eburru GsJj 50, north slope, hilltop, and steam jets"). Obsidian from these different locations might vary in color, texture, or other physical properties. Chemically, however, the obsidian is identical because its expression in different locations seems to represent one volcanic eruption. In addition, based on our fieldwork, we can identify the Eburru and major Naivasha sources as primary, not secondary, obsidian sources. For example, the GsJj 50 locale is a primary exposure that covers an area  $\sim 200 \times 20$  m, and other Eburru locales are similar. The Naivasha sources are more variable. Some sources are obsidian flows that extend nearly 2000 m, whereas others are exposures ~200-800 m<sup>2</sup> in area. Occasionally a source is exposed in only spot or across an entire hillside, leading to a colluvial scatter no more than a few hundred meters in size. Sparse Quaternary rivers cutting through the southern Kenya Rift or draining into Lake Victoria mean that there were few, if any, opportunities for obsidians to be spread across large areas.

Brown et al. (2013) tend to be "splitters" rather than "lumpers" when chemically defining sources. If, for example, two obsidian specimens differ by more than one standard deviation for any of five key elements (i.e., Al, Fe, Ca, Cl, Ti), they defined them as different sources (Brown et al., 2013:3235). Sometimes Brown et al. (2013) defined a source on the basis of only a handful of specimens, occasionally just one or two. This reflects, in part, the challenges of collecting specimens on such an obsidian-rich landscape.

Because we use their data in this paper, we follow the sources as chemically defined by Brown et al. (2013), except when elements we favor (i.e., Zr, Rb, Nb, Sr, Fe, Mn) imply no appreciable difference exists between two sources. Accordingly, the "GsJj 50" locale is not distinguished from other nearby outcrops with obsidian chemically assigned to the "Eburru" source; however, our observations suggest that such distinctions may be possible based on variability in color and texture. Greater specificity might also eventually be possible using quantitative means. In particular, we have sampled the Mt. Eburru obsidian quarries and outcrops with sufficient intensity such that we might be able to quantify spatial differences using rock magnetic characterization (Frahm and Feinberg, 2013a).

It should be stressed that here "pXRF" refers to the handheld instruments about the size, shape, and mass of a cordless drill. Some (e.g., Craig et al., 2007; Liritzis and Zacharias, 2011) consider "pXRF" to include small benchtop instruments that, indeed, have been used to good effect (e.g., Cecil et al., 2007; Liritzis, 2008). Our focus here, however, is the class of ruggedized instruments that can be used equally well in a museum or in the field. It should also be emphasized that pXRF technologies have advanced so much that any performance appraisals more than a few years old are essentially obsolete (e.g., Cesareo et al., 2008; Potts and West, 2008; Williams-Thorpe, 2008; Pessanha et al.,

2009). The X-ray detectors and associated electronics found in a recent pXRF instrument are more sensitive than those in most benchtop models five or ten years ago (Speakman and Shackley, 2013). For example, after a 40-second measurement using our instrument, the detection limit for Sr and Rb was 1–2 ppm for flaked surfaces (i.e., not polished or powdered) of obsidian.

The list of settings where pXRF has been successfully employed in obsidian sourcing has grown markedly in recent years. It has been used, for example, in Eurasia (e.g., Frahm, 2007, 2013, 2014a; Carter, 2009; Jia et al., 2010, 2013; Tykot et al., 2011, 2013; Forster and Grave, 2012; Frahm and Feinberg, 2013b, c; Adler et al., 2014; Frahm et al., 2014a, b, c; Milić, 2014), Oceania (e.g., Golitko et al., 2010, 2012; Sheppard et al., 2010, 2011; Burley et al., 2011; Golitko, 2011; McCoy et al., 2011, 2014; Torrence et al., 2012; Galipaud et al., 2014; Lawrence et al., 2014; Mulrooney et al., 2014), North America (e.g., Millhauser et al., 2011, 2015; Goodale et al., 2012; Mills et al., 2013; Moholy-Nagy et al., 2013; Rodríguez-Alegría et al., 2013; Ebert et al., 2014; Frahm and Feinberg, 2015; Reimer, 2015), and South America (e.g., Craig et al., 2010; Vázquez et al., 2012; Williams et al., 2012; Kellett et al., 2013).

#### 4. Dataset compatibility: what is good enough?

Demonstrating compatibility of our pXRF dataset with those of Brown et al. (2013) is crucial to establishing confidence in our findings. To avoid judgmental determinations of data compatibility, we quantitatively compared obsidian datasets reported in the literature, especially when researchers found them in sufficient agreement to use together.

In one example, Glascock (1999) reports the datasets from a "round robin" in which eight laboratories submitted their values for Sierra de Pachuca (Hidalgo, Mexico) and Little Glass Buttes (Oregon, USA) obsidians (Table 1). The labs used varied analytical techniques (e.g., EDXRF, WDXRF, NAA, ICP-MS, PIXE/PIGME) and, in turn, approaches to calibration, increasing the variability among them. The use of pXRF to characterize Little Glass Buttes obsidian yielded values with above-average accuracy relative to the other datasets (i.e., 7% difference relative to the mean values for all datasets, which, on average, had 11% relative difference; Frahm and Feinberg, 2015). Use of obsidian standards characterized with NAA at MURR also means that the pXRF measurements exhibited good agreement (9% relative difference on average) with the MURR dataset (Table 2), while researchers using different calibrations report values with greater disparities (>16% difference on average). When the highest and lowest disparities are ignored, the pXRF data agree with the MURR NAA data almost as well as the MURR EDXRF data do (6% vs. 4% on average, respectively). Glascock (2011) argues that, for elements of interest, MURR "data on obsidian samples measured by XRF can be compared directly to [data] collected by NAA" (191). This suggests a difference ~5% relative, on average, would be sufficient for compatible datasets.

In a second example, Shackley (2012b) contends, regarding EDXRF in three North American obsidian sourcing labs, that "most of the measurements are within 1%" (see also "often only 1%" in Shackley, 2011a:33). Published measurements from these facilities do not support such claims (Table 3). Instead, data for the RGM-1 obsidian standard, averaged over ten publications, vary with an overall mean of 6% relative. The individual datasets can differ overall by 4 to 9% relative averaged across seven trace elements. Only Zr exhibits an average difference of 1% among the datasets, followed by Rb and Fe (3%). Clearly, though, the Berkeley Geoarchaeological XRF Lab had sufficiently consistent data that source values from one analytical session could be compared to artifact data from another. Furthermore, Shackley (2012b) states that these laboratories routinely use each other's data. It is clearly the case that a standard of "within 1%" is both unrealistic and unnecessary.

In summary, a goal of 5% or less relative difference between datasets is achievable and certainly sufficient for compatible values, whereas a relative difference of 10% or less, at least for certain elements, is likely still sufficient for dataset compatibility. We show that our pXRF data attain such agreement with those in Brown et al. (2013). Seeking to attain even higher dataset agreement (e.g., ≤1%) is impractical. As established in Table 3, EDXRF variability is rarely better than 4% relative over time, even with the same instrument in the same laboratory following the same analytical procedures. Furthermore, concentrations of trace elements can vary slightly within an individual obsidian source. In a pioneering study on this subject, Laidley and McKay (1971) sampled Big Obsidian Flow (Newberry Volcano, Oregon, USA) at 30-m intervals across a 1500-m transect. Their WDXRF data revealed that, while statistically insignificant for most elements, elemental concentrations varied by more than the analytical uncertainties. For example, Rb had an uncertainty of 1.4% relative, but it varied by 3.1% relative across the transect. Furthermore, elements such as Fe, Ti, and Ca all varied by 1–2% relative across the flow. Consequently, striving for <1-2% relative difference between datasets is, in most instances, statistical overkill.

#### 5. Analytical conditions

Here we report the details of our pXRF instrument, its operation, how the raw data were corrected for various physical effects within specimens, and the factory-set calibration which we "fine tuned" for direct compatibility with the published Brown et al. (2013) values.

**Table 2**The pXRF data in Frahm and Feinberg (2015) were calibrated, in part, using NAA and EDXRF data from the University of Missouri's Research Reactor (MURR) for a series of matched obsidian specimens. This yields greater compatibility with MURR datasets (i.e., a lower relative difference) than other calibration approaches in other recent publications.

	Sierra de Pachuca	, Mexico		Little Glass Buttes	, Oregon, U	nited State	s					
	Glascock, 1999	Glascock,	2011	Glascock, 1999	Frahm a Feinberg		Millhau al., 2015		Millhau al., 2011		Scharlotta, 2010	
	MURR	MURR		MURR	Minnes	ota	Field M	useum	Field Mu	ıseum	IIRMES	
	NAA	EDXRF	%Diff	NAA	pXRF	%Diff	pXRF	%Diff	pXRF	%Diff	LA-TOF-ICP-MS	%Diff
Ba	30			1270	1265	0	904	34	776	48	1173	8
Ca					5878				5134		2652	
Fe	15,800	15,900	1	6200	5939	4	5713	8	5408	14	5353	15
Mn	1149	797	36	327	337	3	272	18	227	36	299	9
Nb		84			8				6			
Rb	192	189	2	95	94	1	100	5	101	6	79	18
Sr		10		78	78	0	73	7	73	7	45	54
Ti		945			778				572		420	
Zn	191	207	8	31	38	20	26	18	32	3	27	14
Zr	888	957	7	118	85	33	93	24	91	26	64	59
Mean:			11			9		16		20		25
Trimm	ed mean:		4			6		15		18		22

Table 3
Element values for the powdered obsidian standard RGM-1 (U.S. Geological Survey Glass Mountain rhyolitic obsidian) from laboratories in the United States that offer obsidian sourcing as an analytical service. Shackley (2012b) claims that, for these laboratories, "most of the measurements are within 1%" (also "often only 1%" in Shackley, 2011a:33). However, data from these publications vary with an overall mean of 6% relative. Individual datasets can differ overall, on average, by 4 to 9% relative. Only Zr has an average difference of 1% among the datasets, followed by Rb and Fe (3%).

	Cited in Sha	ckley, 2012b							Other Berkel	ey data		
	Speakman a	nd Shackley, I	2013	Skinner a 1996	nd Davis,		Hughes, 200	)7	Negash and Shackley, 20	06	Carter and Sha 2007	ickley,
	Berkeley	Georgia (	CAIS	NW Obsid	lian	_	Geochem Re	<u></u>	Berkeley		Berkeley	
	Mean	Mean	%Diff	Mean	%Dif	ff	Mean	%Diff	Mean	%Diff	Mean	%Diff
Mn	302	321	6	291		4	278	8	308	2	278	8
Fe	13,116	13,075	< 1	13,480		3	13,079	< 1	13,988	6	14,212	8
Rb	151	157	4	152		1	143	5	154	2	153	1
Sr	106	104	2	107		1	105	1	113	6	114	7
Y	25	26	4	24		4	23	8	22	13	23	8
Zr	219	223	2	217		1	214	2	224	2	221	1
Nb	9	10	11	11		20	8	12	8	12	9	<1
Mean:			4			5		5		6		5
Trimmed:			4			2		5		6		5
			Other Berk	eley data								
			Shackley, 2	2009	Craig et a	l., 2007	Dillian	et al., 2010	Ogburn	et al., 2009	Doroniche Shackley, 2	
			Berkeley		Berkeley		Berkel	ley	Berkele	У	Berkeley	
	Overall avera	age %Diff	Mean	%Diff	Mean	%Diff	Mear	n %Diff	Mean	%Diff	Value	%Diff
Mn		6	292	3	340	12	313	3 4	322	6	296	2
Fe		3	12,806	2	13,251	1	13,299	9 1	12,778	3	13,676	4
Rb		3	145	4	152	1	148	3 2	148	2	143	5
Sr		4	103	3	112	6	110	) 4	102	4	104	2
Y		8	23	8	20	22	22	2 13	25	<1	26	4
Zr		1	221	1	223	2	218	< 1	213	3	220	<1
Nb		14	7	25	9	<1	$\epsilon$	5 40	10	11	10	11
Mean:		6		7		6		9		4		4
Trimmed:		5		4		4		5		4		3

**Table 4**List of 27 obsidian specimens from Brown et al. (2013) analyzed by pXRF for this study. The first twelve specimens were used to calibrate the instrument, while the second batch of fifteen was measured for reproducibility checks.

Specimen	Merrick & Brown	Brown et al., 2013				
	Chemical Type	Source/location	Source group/area	Source region	N. Lat.	E. Long.
Calibration st	andards, n = 12					
MER 31	Type 20	Hell's Gate #1	Ol Karia Group, South Naivasha	Naivasha-Nakuru	-0.88	36.34
MER 36	Type 8	Kisanana	Kisanana and Mugerin	Mt. Kenya/Baringo	0.03	36.06
MER 40	Type 9	Kabazi	Kampi ya Moto, Kabazi, Rigo Cave	Mt. Kenya/Baringo	-0.08	36.17
MER 42	Type 11	Mackinder #2	Mackinder Valley, Mt. Kenya	Mt. Kenya/Baringo	-0.12	37.29
MER 63	Type 6	Karau, Lake Baringo Region	Karau, Kampi ya Samaki, Lokoritabim	Mt. Kenya/Baringo	0.62	36.19
MER 65	Type 6	Karau, Lake Baringo Region	Karau, Kampi ya Samaki, Lokoritabim	Mt. Kenya/Baringo	0.62	36.19
MER 68	Type 14	Gicheru Diatomite Quarry	South Kenya Rift Valley	Southern Kenya	-1.19	36.55
MER 71	Type 32	Ilkek	Mt. Eburru, West Lake Naivasha	Naivasha-Nakuru	-0.59	36.37
MER 74	Type 35	Opuru	Mt. Eburru, West Lake Naivasha	Naivasha-Nakuru	-0.59	36.25
MER 80	Type 15	Magadi East	South Kenya Rift Valley	Southern Kenya	-1.82	36.30
MER 82	Type 20	Njorowa Gorge South	Ol Karia Group, South Naivasha	Naivasha-Nakuru	-0.96	36.31
MER 113	Type 53	Kijabe Escarpment Road	-	Southern Kenya	-1.08	36.60
Reproducibili	ty checks, n = 15					
MER 34	Type 22	Akira Ranch	-	Southern Kenya	-0.99	36.31
MER 38	Type 9	Kampi ya Moto #2	Kampi ya Moto, Kabazi, Rigo Cave	Mt. Kenya/Baringo	-0.11	35.95
MER 45	Type 12	Mangu	=	Southern Kenya	-1.00	36.95
MER 69	Type 14	Gicheru Diatomite Quarry	South Kenya Rift Valley	Southern Kenya	-1.19	36.55
MER 70	Type 32	Ilkek	Mt. Eburru, West Lake Naivasha	Naivasha-Nakuru	-0.59	36.37
MER 75	Type 35	Ориги	Mt. Eburru, West Lake Naivasha	Naivasha-Nakuru	-0.59	36.25
MER 76	Type 27	Cedar Hill South	Mt. Eburru, West Lake Naivasha	Naivasha-Nakuru	-0.61	36.27
MER 83	Type 20	Njorowa Gorge South	Ol Karia Group, South Naivasha	Naivasha-Nakuru	-0.96	36.31
MER 96	Type 24	Kinangop Escarpment	Ol Karia Group, South Naivasha	Naivasha-Nakuru	-0.63	36.49
MER 99	Type 31	West Naivasha #1	Mt. Eburru, West Lake Naivasha	Naivasha-Nakuru	-0.69	36.31
MER 105	Type 12	Chania Dam	=	Southern Kenya	-0.88	36.84
MER 112	Type 53	Kijabe Escarpment Road	=	Southern Kenya	-1.08	36.60
MER 115	Type 29	Upper Eburru, North Slope	Mt. Eburru, West Lake Naivasha	Naivasha-Nakuru	-0.62	36.25
MER 117	Type 29	Upper Eburru, Hilltop	Mt. Eburru, West Lake Naivasha	Naivasha-Nakuru	-0.63	36.26
MER 119	Type 29	Upper Eburru, Hilltop	Mt. Eburru, West Lake Naivasha	Naivasha-Nakuru	-0.63	36.26

#### 5.1. Instrument and settings

Our analyses used a Thermo Scientific Niton XL3t GOLDD instrument. To generate incident X-rays, it has a miniaturized 50-kV, Ag-anode X-ray tube. The tube's voltage and current vary in combination with different X-ray filters during a measurement to optimally fluoresce different

portions of the periodic table. The operating conditions were 40 kV and  $\leq\!50~\mu\text{A}$  with the "main" X-ray filter, 20 kV and  $\leq\!100~\mu\text{A}$  with the "low" filter, and 50 kV and  $\leq\!40~\mu\text{A}$  with the "high" filter. As is the case with many modern XRF instruments (Shackley, 2011a), the instrument adjusts the tube current automatically to attain optimal X-ray count rates. To measure the X-rays emitted by a specimen, this instrument is

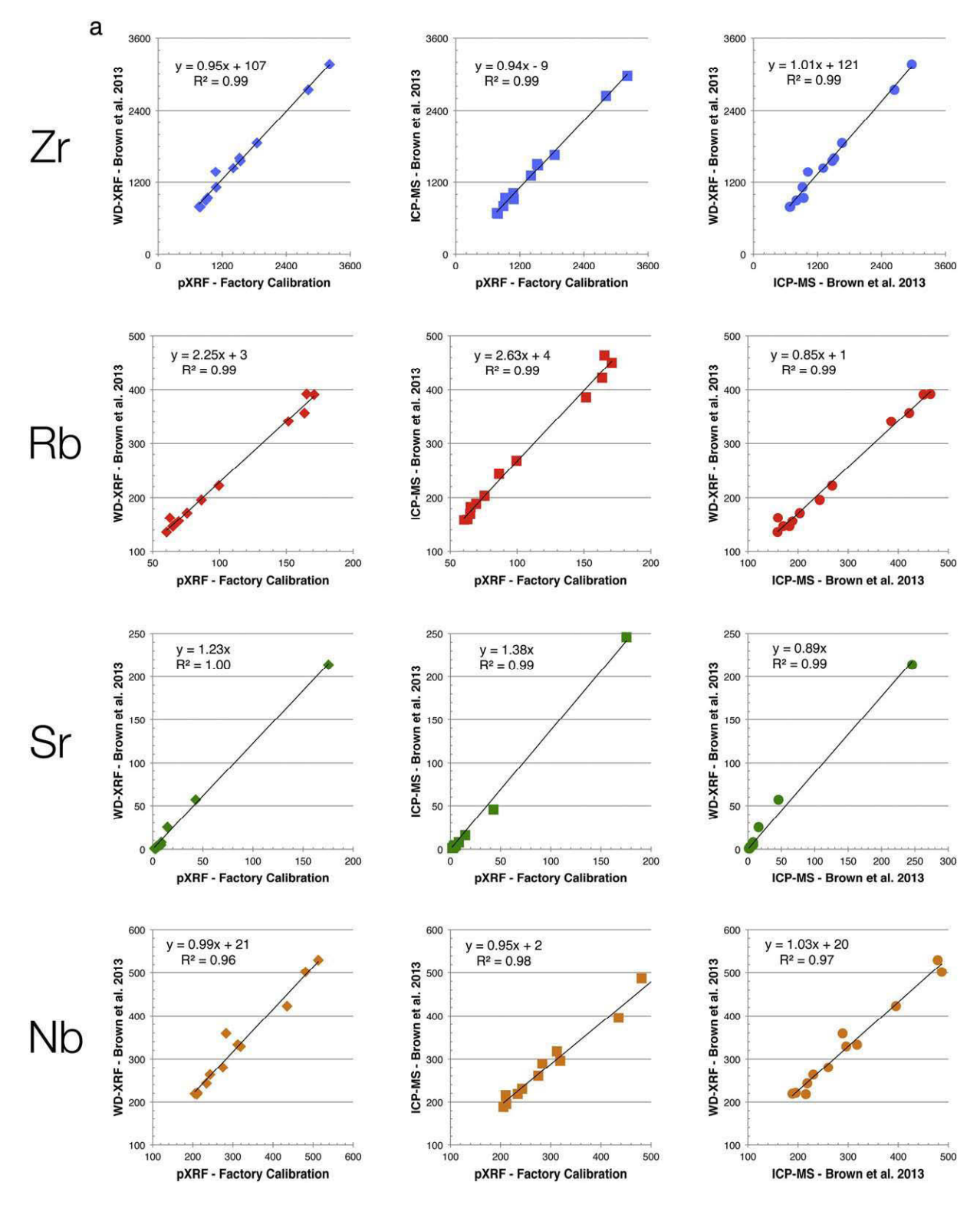


Fig. 3. Best-fit lines and correlations (i.e., R<sup>2</sup>) between our pXRF (with initial factory-set calibration) data and the published datasets from Brown et al. (2013) for a set of twelve matched obsidian specimens (Table 4): pXRF versus WDXRF (diamonds), pXRF versus EMPA (triangles), pXRF versus ICP-MS (squares), and WDXRF and EMPA versus ICP-MS (circles). These equations were used to calibrate our pXRF data to the other datasets. In this case, we calibrated our pXRF data to those from Brown et al. (2013).

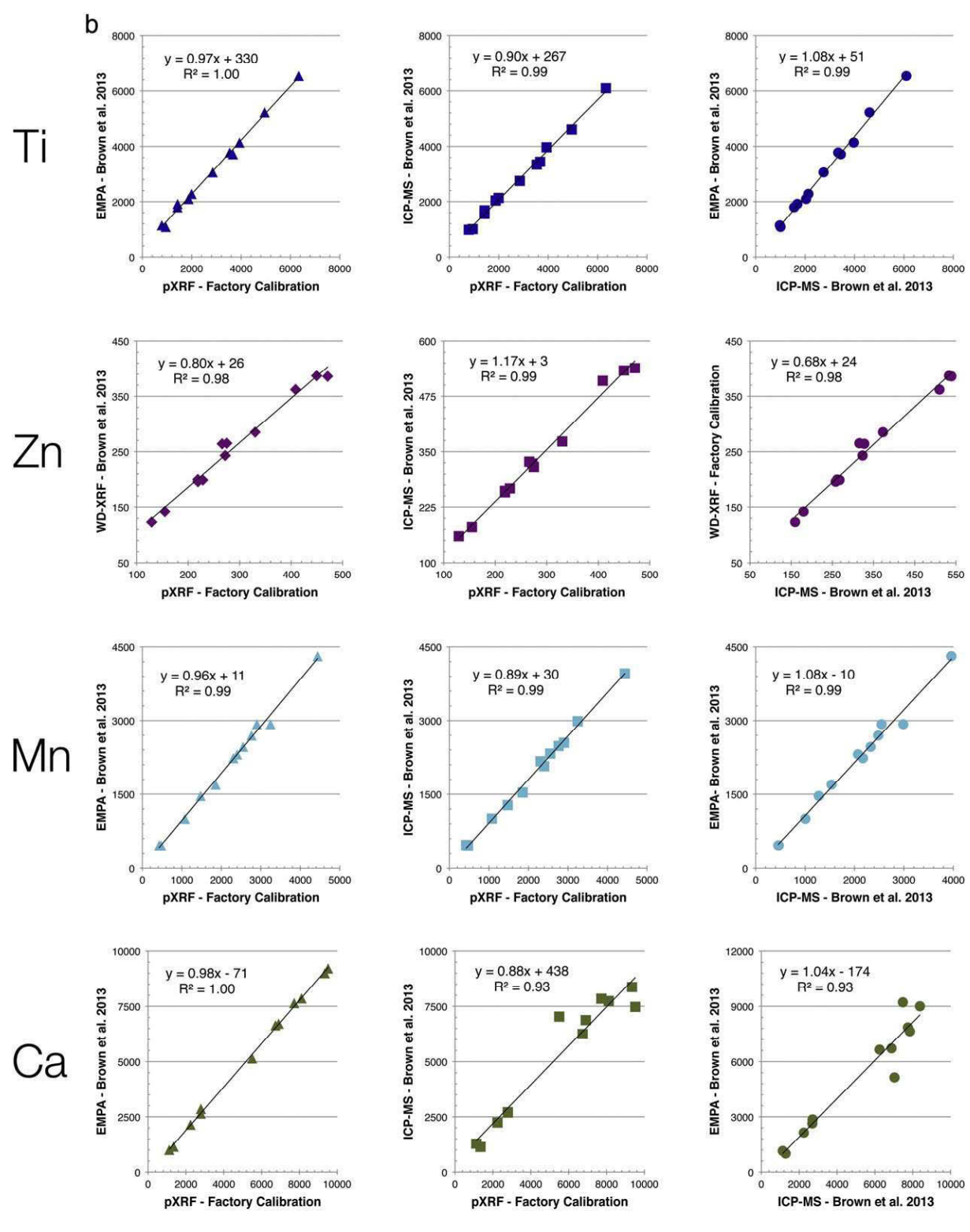


Fig. 3 (continued).

outfitted with a 25-mm² Si drift detector (SDD) that has an energy resolution  $\leq$  155 eV in practice. Ordinarily the X-ray beam is ~8-mm in diameter (~50 mm²), but the instrument is also equipped with a small-spot collimator that can restrict the beam to a ~3-mm diameter (~7 mm²), yielding an analytical area ~85% smaller, well suited for small (<5 mm) artifacts. Measurements with the full-size beam were 120 s (40 s each for three filters), whereas those with the small spot were 90 s (45 s

each for two filters). The instrument was mounted in a portable Thermo Scientific SmartStand for the most precise positioning of the geological specimens and artifacts. Although this instrument is equipped to measure >40 elements (including, except for Na, all major elements in obsidians), our focus was a subset of elements well measured both by pXRF and by the techniques used by Brown et al. (2013) since not all techniques have equal sensitivities for all elements.

#### 5.2. Correction scheme

Measured X-rays must be "corrected" for a variety of physical phenomena, including inter-element effects, within a specimen (e.g., Xray absorption and attenuation, secondary and tertiary X-ray fluorescence, photoelectric emission). There are several approaches to correction: empirical methods (e.g., alpha factors, influence coefficients), normalization to a certain phenomenon (e.g., Compton scattering), or physics-based models (e.g., fundamental parameters). We use the fundamental parameters (FP) approach, which, for each analysis, solves a set of nonlinear equations that describes the relationship between Xray emission intensities and elemental concentrations in a given specimen. FP correction has been used routinely in select XRF applications since the 1990s (de Boer and Brouwer, 1990). Because FP correction involves more intensive calculations than empirical methods (e.g., influence coefficients date back to the 1950s; Sherman, 1955), the addition of powerful processors to pXRF instruments has allowed its implementation. Heginbotham et al. (2010) conducted an inter-laboratory test based on 12 copper alloys measured by 19 different XRF instruments and methods in 14 laboratories worldwide. The single greatest variable in accuracy was the correction scheme. All of the highest ranked instruments used FP calibrated with standards, whereas instruments with empirical correction approaches ranked lower. Heginbotham et al. (2010: 185) report that "it is very clear that laboratories using fundamental parameters software calibrated with standards... performed consistently more accurately than laboratories using other methods," despite each of the top-performing labs using different models and brands. Our choice of calibration standards, specifically a collection of matched Kenyan obsidian specimens from Brown et al. (2013), is discussed in Section 6.

#### 5.3. Initial factory-set calibration

Like all modern pXRF instruments from major manufacturers, the instrument has a factory-set calibration. In fact, it has two "internal" calibrations: one for its "mining" mode and one for its "soils" mode. Both calibrations are intended to be flexible and remain stable for a long time. The "mining" calibration is principally geared toward various applications in mining and geological exploration, while the "soils" calibration is optimized to measure soil contaminants in environmental testing and remediation. These factory-set calibrations are tested for accuracy against a set of certified standard reference materials (SRM), largely from the United States' National Institute of Standards and Technology (NIST). The Thermo engineers assessed the "mining" calibration with six metal and phosphorous ores (e.g., NIST SRMs 25d, 113b, and 694) as well as feldspar (NIST SRM 70a). These factory calibrations can yield accurate values for a few elements in obsidian but inaccurate values for others. Given that these calibrations are intended to be broadly applicable across a wide range of values, it is not surprising that, for the narrow concentration ranges in obsidians, further calibration is needed. Fortunately, it is straightforward to adjust the factory-set calibrations using linear regression, as shown here, thereby forming the basis of our custom calibration specifically tailored to the datasets in Brown et al. (2013).

#### 6. Calibration approach

There are two approaches to XRF calibration for obsidian artifact sourcing. The two approaches are conceptually similar, and the only significant difference is the compositional range of the standards. In this study, we used a set of obsidian specimens from Brown et al. (2013) as calibration standards to "fine-tune" our data specifically and directly to theirs. As demonstrated in Section 7, this approach yielded directly compatible datasets.

#### 6.1. Two calibration approaches

The first strategy is to create a generalized silicate or volcanic rock calibration based on a collection of certified SRM powders, often principally from the United States Geological Survey (USGS). This calibration approach has been favored at Berkeley's Geoarchaeological XRF Laboratory (e.g., Shackley, 1995, 2005, 2011b) and McMaster's Archaeological XRF Lab (e.g., Carter and Contreras, 2012; Carter et al., 2013), among other XRF labs. Only three of Shackley's (2011b) sixteen standards are obsidians (e.g., USGS RGM-1), and the remaining SRMs fall outside the usual compositional range for rhyolitic obsidians and include basalts, andesites, and other volcanics (e.g., USGS AGV-2 and BHVO-2) as well as metamorphic and sedimentary rocks (e.g., USGS SDC-1 and SCO-1). The result is a calibration that is effective for obsidian but also generally applicable to a broader range of volcanic rocks (e.g., Shackley, 2011b, 2012a). The key advantage is that, other things being equal, analytical facilities that calibrate using similar sets of USGS SRMs should produce data having the greatest possible compatibility with the USGS and, consequently, with each other.

The second approach is to calibrate an XRF instrument using a collection of obsidian specimens that have been characterized using several analytical techniques (often NAA and one or two others). This strategy has been favored by MURR (e.g., Glascock, 2011; Ferguson, 2012; Glascock and Ferguson, 2012) and the lead author (e.g., Frahm and Feinberg, 2013b, c, 2015; Frahm, 2014a; Frahm et al., 2014a, b, c), among others. For example, MURR assembled a set of 40 obsidian specimens from American sources and determined their compositions with NAA and two ICP-MS methods as a means to calibrate XRF instruments. When plotted on a total alkali vs. silica (TAS) plot and classified according to Le Maitre et al. (2002), most of the obsidians are rhyolitic (n =35), four are trachytic, and one is an andesitic basalt. This calibration set reflects the compositions of American obsidians, which are predominantly rhyolite (Hughes and Smith, 1993; Glascock, 1994; Shackley, 2005). Shackley (2011a:34) notes that, when selecting calibration standards, "they should exhibit the entire range of variation expected from the rocks to be analyzed." Thus, for typical rhyolitic obsidians, XRF data calibrated using these standards will maximize reproducibility with respect to MURR's NAA and ICP-MS datasets. Similarly, Frahm (2014a) describes a series of 24 obsidian standards from Southwest Asia (i.e., Armenia, Georgia, and Turkey), all rhyolitic, analyzed by NAA and XRF at MURR and EMPA at Minnesota. The resulting pXRF data exhibit high reproducibility with respect to MURR and Minnesota data for rhyolitic obsidians, from Armenia (e.g., Frahm, 2014a; Frahm et al., 2014b) to the Americas (Frahm and Feinberg, 2015).

#### 6.2. Issues with past approaches

A key aspect of this study was attaining the greatest possible compatibility with the Kenyan obsidian sources' compositional data in Brown et al. (2013). Accordingly, it did not make sense, with this goal, to calibrate to SRMs from the USGS and other organizations, nor could we simply calibrate with the standards used to generate these datasets. For instance, calibration for EMPA is commonly different than that for XRF. EMPA calibration ordinarily involves a single standard per element, and typically only the major elements are calibrated on a standard close in composition to the unknowns. Thus, Brown et al. (2013) calibrated for Si, Al, and K with their in-house Mineral Mountain obsidian standard, whereas Zr, Ti, and Fe were calibrated with their oxides: ZrO<sub>2</sub>, TiO<sub>2</sub>, and Fe<sub>2</sub>O<sub>3</sub>, respectively. Calibration for ICP-MS used a single standard: NIST SRM #610, a synthetic glass. The WDXRF calibration used three standards: USGS G-2 (granite powder, which is no longer available) for Sr and two in-house standards for the other elements. Furthermore, while their EMPA procedures have undergone extensive accuracy testing (e.g., Jochum et al., 2006: Lab 28; Kuehne et al., 2011: Lab 5), we do not have similar assessments of their WDXRF and ICP-MS data. Brown et al. (2013) did, though, compare the WDXRF and ICP-MS datasets and establish, for example, that WDXRF consistently measured ~85 ppm of Rb for every 100 ppm measured by ICP-MS, meaning that both sets of Rb values cannot be entirely accurate.

Nor was it appropriate to simply use a set of standards based on rhyolitic obsidians from Southwest Asia (e.g., Frahm, 2014a; Frahm et al., 2014b) or the Americas (e.g., Glascock, 2011; Glascock and Ferguson, 2012). As reported by Brown et al. (2013), Kenyan obsidians span much of the compositional range of igneous rocks from rhyolite to phonolite. Based on the compositional analyses summarized by Brown et al. (2013), two-thirds (66%) of the Kenyan obsidian specimens are rhyolitic. The rest are phonolite (18%) and trachyte (16%), according to a TAS plot. Even the rhyolitic obsidians have elemental concentrations outside typical ranges. For example, of their rhyolitic specimens, half (51%) have FeOtotal above 7 wt.%, almost two-thirds (62%) have Mn above 1000 ppm, most (92%) have Zr above 1000 ppm, and most (90%) have Nb above 200 ppm. These concentrations are outside typical rhyolitic obsidian variability (e.g., Glascock, 1994; Ferguson, 2012), and Shackley (2011a) emphasizes a need for standards to reflect unknowns' full compositional range. Indeed, Ferguson (2012) mentions issues encountered by MURR (e.g., too low Zr and Nb values) when their custom Americas-based obsidian calibration was applied to Kenyan obsidians.

#### 6.3. Matched specimens as standards

To maximize compatibility with the obsidian data in Brown et al. (2013), we used a set of 27 obsidian specimens originally analyzed for their study (Table 4), provided to us by Frank Brown. Therefore, we were able to match their data to ours for the same specimens without any uncertainties regarding different source terminology or other potential sources of variation. Twelve of the specimens were selected for use as calibration standards. They were measured using the instrument's factory-set "mining" calibration (see Section 5.3), our values were compared to those of Brown et al. (2013), and linear regression was used to derive calibration equations (Fig. 3). The other fifteen specimens served as independent "secondary standards" to assess the

custom calibrations and to demonstrate how well our calibrated pXRF data can replicate values in Brown et al. (2013). Thus, our standards in this study are specifically tailored not only to the chemical range of Kenyan obsidians but also the measurements of Brown et al. (2013), regardless of their accuracy.

Table 5 shows the WDXRF, ICP-MS, and EMPA data from Brown et al. (2013) for the twelve calibration standards. It also shows our pXRF measurements with the initial factory-set calibration. Fig. 3 shows the linear regression analyses of these datasets. These plots illustrate the correlations between the data from WDXRF and pXRF (diamonds), EMPA and pXRF (triangles), ICP-MS and pXRF (squares), and WDXRF or EMPA and ICP-MS (circles) in Table 5. Note that the correlations between the datasets are often very high (i.e., R² is often 0.98 or better), which is paramount for their compatibility. In fact, as shown in Fig. 3, the pXRF data are as highly correlated to the datasets in Brown et al. (2013) as the Brown et al. (2013) datasets are to each other. We used the equations of these best-fit lines to calibrate our pXRF data specifically to the measurements of Brown et al. (2013).

#### 7. Evaluating compatibility between datasets

Once the calibrations based on twelve obsidian specimens from Brown et al. (2013) were applied to our pXRF measurements, the remaining fifteen specimens from Brown et al. (2013) were used as independent "secondary standards" to check the reproducibility and to demonstrate that our measurements are compatible with theirs. First, we plot the values to find the correlations between datasets as well as the slopes of the best-fit lines. Second, we calculate the percent relative difference between the measurements.

#### 7.1. Plotting correlation and slope

Fig. 4 shows the checks for our pXRF data calibrated to their WDXRF and EMPA data. The correlations for these elements are high, particularly Zr ( $R^2 = 0.99$ ), Fe (0.99), Rb (0.98), Ti (0.98), Nb (0.96), and Ca (0.96).

**Table 5**Brown et al. (2013) values (EMPA, WDXRF, ICP-MS) used for calibration and pXRF values using the initial factory-set calibration.

	Zr			Rb			Sr			Nb			Fe	
	WDXRF	ICP-MS	pXRF <sup>a</sup>	EMPA	pXRF <sup>a</sup>									
MER 31	1607	1512	1523	392	464	165	1	2	3	333	318	312	29,400	26,543
MER 36	1860	1661	1851	222	268	100	25	16	15	502	487	481	70,700	69,277
MER 40	899	806	892	157	189	69	1	1	2	243	218	234	68,040	71,166
MER 42	1374	1020	1077	163	160	63	214	246	175	359	289	283	41,720	44,034
MER 63	795	692	769	147	171	65	3	4	4	219	189	206	57,470	57,246
MER 65	793	680	790	147	183	65	3	3	4	221	195	211	57,330	58,958
MER 68	1117	921	1088	196	243	86	57	46	43	263	230	243	23,870	24,056
MER 71	2740	2640	2813	357	422	164	5	8	8	423	395	435	54,740	55,865
MER 74	1437	1307	1407	172	203	76	1	3	3	280	260	275	73,500	71,149
MER 80	940	942	926	136	159	60	3	5	5	218	216	210	65,800	64,744
MER 82	1562	1476	1541	391	450	171	3	4	4	329	296	319	26,950	27,833
MER 113	3165	2966	3211	341	386	152	8	8	9	530	479	513	38,850	40,501
	Ti			Zn			Mn			Ca			K	
	EMPA	ICP-MS	pXRF <sup>a</sup>	WDXRF	ICP-MS	pXRF <sup>a</sup>	EMPA	ICP-MS	pXRF <sup>a</sup>	EMPA	ICP-MS	pXRF <sup>a</sup>	EMPA	pXRF <sup>a</sup>
MER 31	1140	976	785	264	327	266	462	468	425	1000	1284	1123	38,263	29,641
MER 36	2100	2040	1871	387	533	450	4312	3958	4438	6646	6247	6734	37,018	28,942
MER 40	4140	3969	3935	243	323	272	2926	2987	3243	6717	6878	6900	39,508	31,779
MER 42	6540	6095	6334	142	180	155	2233	2170	2303	9004	8377	9337	45,484	36,878
MER 63	3780	3340	3535	196	258	219	2695	2480	2765	7646	7843	7721	45,069	34,801
MER 65	3720	3444	3671	199	267	228	2926	2547	2899	7861	7741	8110	47,476	36,931
MER 68	3060	2748	2849	123	160	129	1001	1005	1076	5145	7037	5500	44,820	35,288
MER 71	1920	1688	1426	386	539	471	1694	1534	1853	2144	2244	2243	38,263	30,824
MER 74	1800	1555	1421	362	510	409	2310	2071	2397	2858	2707	2792	36,022	28,659
MER 80	5220	4606	4951	200	262	219	2464	2327	2551	9218	7475	9513	41,915	34,574
MER 82	1080	1002	946	265	316	275	462	458	471	1143	1133	1346	38,097	29,502
MER 113	2280	2133	1992	285	373	330	1463	1277	1475	2644	2692	2787	40,172	31,876

<sup>&</sup>lt;sup>a</sup> These pXRF values reflect the generic factory-set calibration, not the new calibration based on these obsidian specimens as standards.

Sr has the lowest correlation ( $R^2 = 0.89$ ), but this is partly a result of mostly low concentrations with one high value. The slope (m) of these best-fit lines are mostly near 1 (0.97–1.00), with Sr as the exception (m = 0.94) for the same reason. The overall mean values are  $R^2 = 0.95$  and m = 0.99 for these elements.

Fig. 5 shows similar checks for our pXRF values calibrated to the ICP-MS data in Brown et al. (2013). The correlations are again high, including that for Sr ( $R^2=0.99$ ), which indicates high reproducibility between our pXRF values and their ICP-MS values. Ca has the lowest correlation ( $R^2=0.86$ ) here. With the exception of Sr, the slopes of the best-fit lines are again mostly near 1 (m=0.94-1.01), supporting compatibility. The overall mean values for these datasets are  $R^2=0.95$  and m=0.95, only a slight decrease.

#### 7.2. Calculating percent relative difference

Table 6 shows the WDXRF and EMPA data from Brown et al. (2013) alongside our calibrated pXRF data for these fifteen obsidian specimens.

The percent differences between the measurements are also shown. Note that, because Sr occurs at such low concentrations in these obsidians, the percent relative difference between the datasets is inflated. Horwitz et al. (1980) demonstrated that, for any analytical technique, uncertainties will increase as the element's concentration decreases. With the exception of Sr, the difference between the pXRF and WDXRF data varies, on average, from 2% (Zr) to 5% (Zn). The relative difference between the pXRF and EMPA data are almost as small, varying from 2% (K) to 7% (Ca and Mn), on average. Therefore, our calibrated pXRF data achieve our goal: 5% or less relative difference with respect to the WDXRF data from Brown et al. (2013), and these differences are only slightly greater ( $\leq 7\%$  relative) with respect to the EMPA data.

Table 7 shows the ICP-MS data from Brown et al. (2013) alongside our pXRF data with the corresponding calibration. The relative differences between the measurements are also listed (again Sr has an inflated relative difference due to its low concentrations). With the exceptions of Sr, the difference between the pXRF and ICP-MS values varies, on average, from 5% (Nb, Rb, Zn, and Ti) to 7–8% (Zr and Mn)

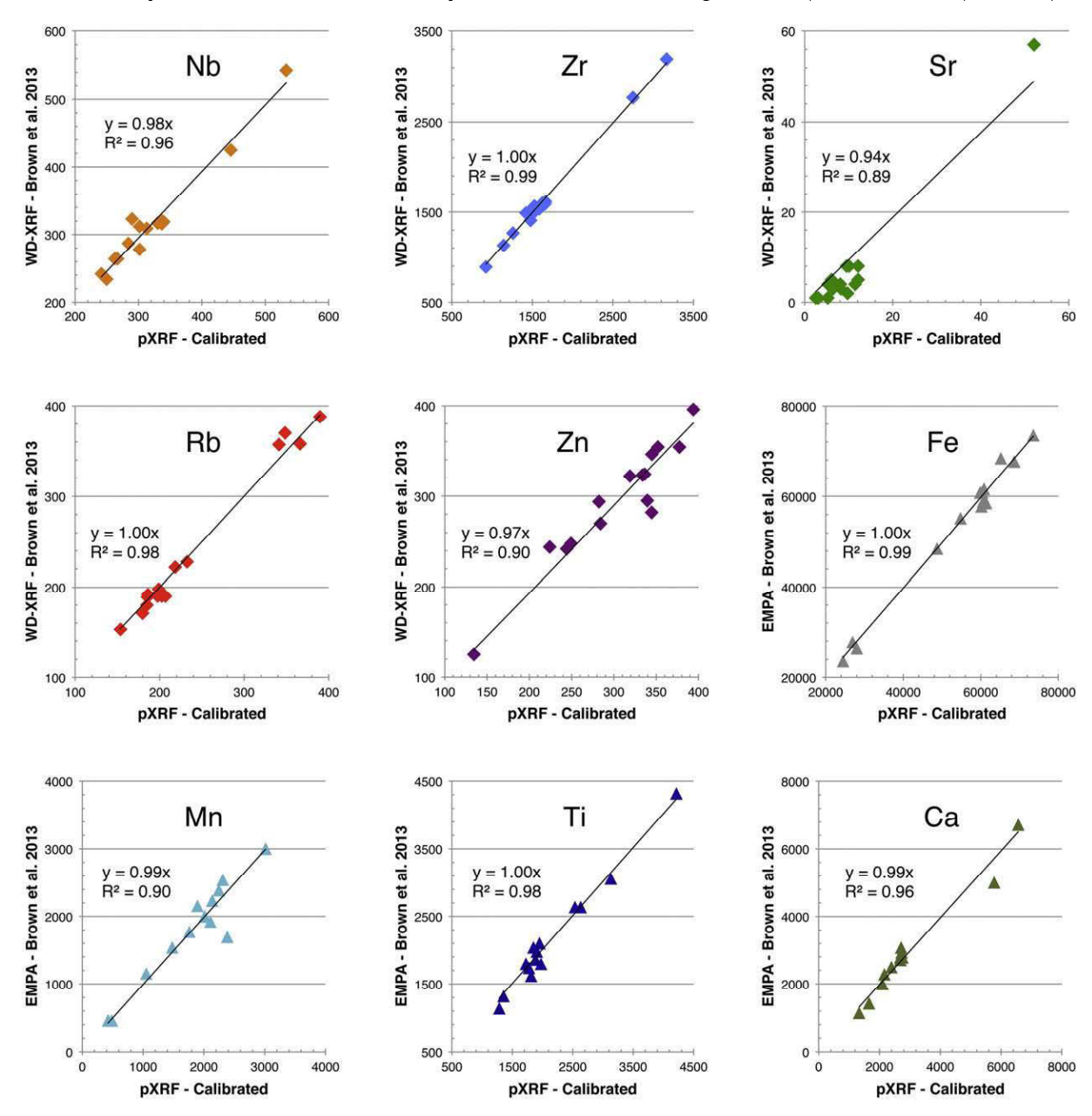


Fig. 4. Best-fit lines and correlations between our pXRF (with our adjusted calibrations from Fig. 3) data and the published WDXRF and EMPA datasets from Brown et al. (2013) for a series of fifteen matched obsidian specimens used as reproducibility checks (Table 4): pXRF versus WDXRF (diamonds) and pXRF versus EMPA (triangles).

to 20% (Ca). While not as excellent as the agreement between the pXRF and WDXRF datasets (2–5%), most elements still exhibit good agreement (5–8% relative) between the pXRF and ICP-MS datasets.

#### 7.3. Summary

Our pXRF values, when calibrated to the WDXRF and EMPA data from Brown et al. (2013), exhibit high compatibility with those datasets. When plotted, their correlations are high (on average,  $R^2=0.95$ ), and the best-fit slopes nearly equal 1 (on average, m=0.99) for the elements of interest. Additionally, the percent relative differences are small: 2–5% with respect to the WDXRF data and 2–7% with respect to the EMPA data. There should be little lingering doubt these datasets can be reliably and validly used together. As a result, we can now use pXRF in combination with the Brown et al. (2013) database as a means to conduct rapid and field-based source identifications of Kenyan obsidian artifacts. This calibration approach is entirely generalizable, not specific to our particular pXRF instrument, model, or brand. Specimens

from a range of Kenyan obsidian sources (with known compositions that span the anticipated chemical range) can be used to similarly calibrate any XRF instrument, regardless of whether it is portable or laboratory-based.

#### 8. Study area: six Winam Gulf rock shelters

We analyzed 78 obsidian artifacts from the Randhore, Rangong, Nyaidha, Jawuoyo, Agoro, and Abindu rock shelters along the northern margins of the Winam Gulf in Kenya (Fig. 2). The sites were originally excavated and reported by Gabel (1969), and portions of these six artifact assemblages are housed at the Gabel Museum of Archaeology at Boston University, USA. We sourced the full collection of obsidian artifacts currently housed in Boston at the Gabel Museum. Our results augment those of Merrick and Brown (1984b), who reported the source attributions of 52 obsidian artifacts from Jawuoyo stored at the National Museums of Kenya in Nairobi. Each rock shelter formed beneath a large Precambrian granitic tor with sediments formed by anthropogenic,

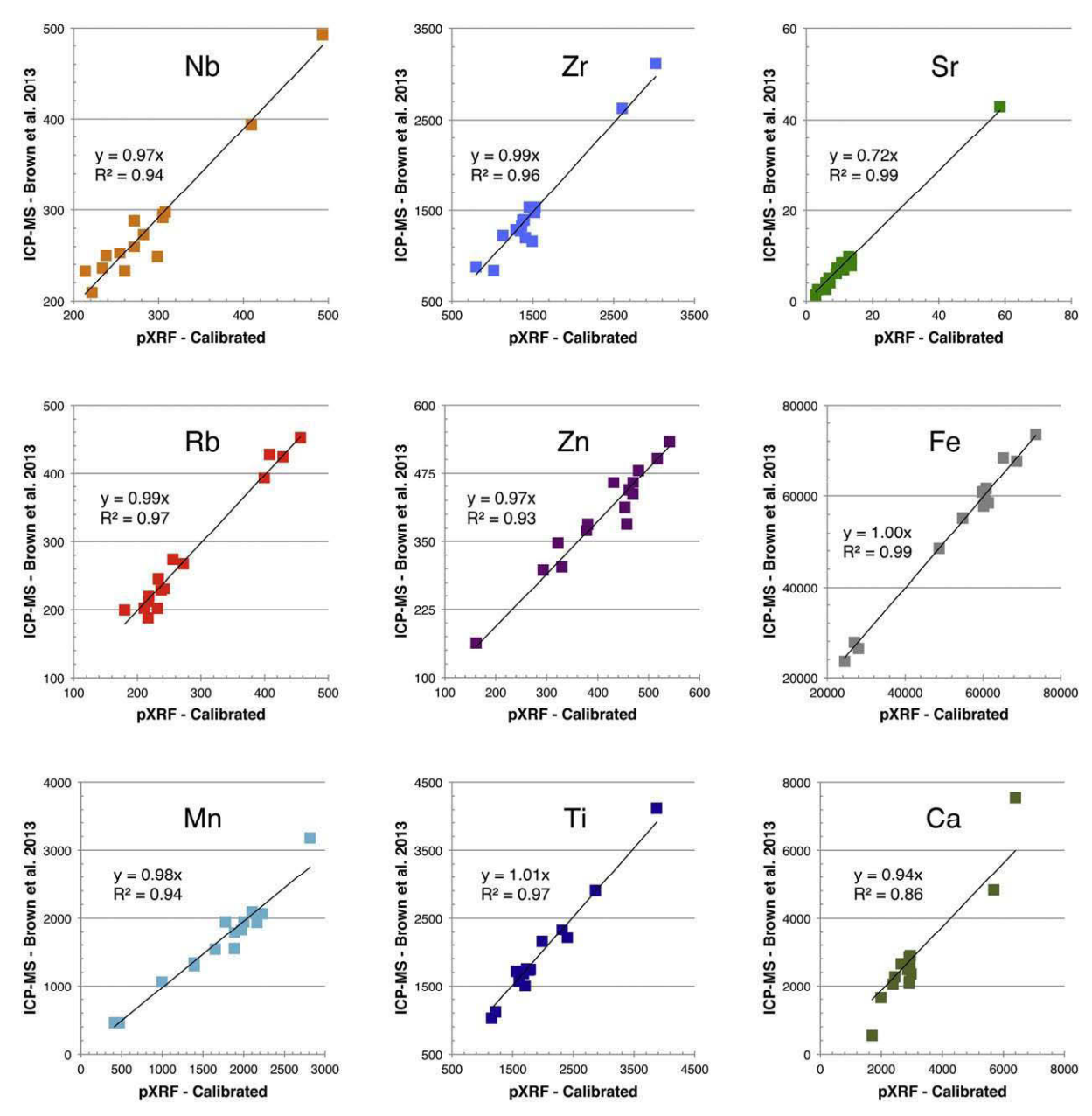


Fig. 5. Best-fit lines and correlations between our pXRF (with our adjusted calibrations from Fig. 3) data and the published ICP-MS datasets from Brown et al. (2013) for a series of fifteen matched obsidian specimens used as reproducibility checks (Table 4).

 Table 6

 Comparison of WDXRF/EMPA data from Brown et al. (2013) to fully calibrated pXRF data for matched obsidian specimens not included in the calibration's linear regression analysis.

	Nb			Zr			Sr			Rb			Zn		
	WDXRF	pXRF (cal)	%Diff	WDXRF	pXRF (cal)	%Diff	WDXRF	pXRF (cal)	%Diff*	WDXRF	pXRF (cal)	%Diff	WDXRF	pXRF (cal)	%Diff
MER 34	312	+	3	1489	+	5	8		23	370	$348 \pm 18$	9	244	+	∞
MER 38	242	$241 \pm 8$	0	890	$923 \pm 31$	4	1	$3\pm1$	98	153	$154 \pm 4$	0	242	244 ± 8	-
MER 45	287	+	-	1565	+	m	5		20	189	+	2	346	+	0
MER 69	264	+	-	1129	+	-	57		6	198	$199 \pm 1$	0	125	+	7
MER 70	425	+	2	2770	+	1	2		132	358	$366 \pm 8$	2	396	+	-
<b>MER 75</b>	278	+	8	1407	+	2	1		136	171	+	2	354	+	9
MER 76	309	$313 \pm 4$	-	1526	+	2	4		89	192	+	3	354	+	-
MER 83	319	+	9	1535	+	3	3		72	388	#	0	248	+	_
<b>MER</b> 96	234	+	7	1483	+	-	1		102	228	+	2	294	+	4
<b>MER</b> 99	264	+	-	1266	+	1	n		93	222	+	2	322	+	-
MER 105	323	+	11	1516	+	2	4		28	180	+	3	323	+	3
MER 112	543	+	2	3193	+	_	8	$10 \pm 1$	17	357	$341 \pm 14$	2	270	+	2
MER 115	320	+	2	1613	+	3	4	11 ± 1	96	190	+	8	282	+	20
MER 117	316	$337 \pm 5$	9	1589	$1656 \pm 20$	4	5	$12 \pm 1$	83	190	+	9	295	+	14
MER 119	317	$330 \pm 3$	4	1598	+	2	8	$12 \pm 1$	41	190		4	324	$336 \pm 11$	4
Mean			4			2			29			3			2
	ı			;			į			(			;		
	re _			MN .			11			Ca			K		
	EMPA	pXRF (cal)	%Diff	EMPA	pXRF (cal)	%Diff	EMPA p	oXRF (cal)	%Diff	EMPA pX	oXRF (cal)	%Diff	EMPA	pXRF (cal)	%Diff
MER 34	27,790	$26,959 \pm 1906$	3	462	+	6	1320	$1355\pm72$	3	1429	$1657 \pm 184$	15	38,678	$36,792 \pm 1999$	2
MER 38	069,690	$68,651 \pm 1766$	1	3003	+	0	4320	+	2	6717	$6566 \pm 299$	2	39,010	$38,949 \pm 1422$	0
<b>MER 45</b>	60,830		2	2387	$2247 \pm 137$	9	2640	$2537 \pm 66$	4	2930	$2727 \pm 163$	7	38,014	+1	3
MER 69	23,590	$24,461 \pm 529$	4	1155	+	6	3060	+	2	5002	$5774 \pm 625$	14	45,069	+	-
MER 70	55,230	$54,478 \pm 1181$	-	1771	+	-	1800	+	4	2001	$2095 \pm 83$	2	38,180	$38,887 \pm 607$	2
<b>MER 75</b>	73,500	$73,566 \pm 935$	0	1694	+	34	1740	+	2	2715	$2683 \pm 23$	-	36,271	+	33
<b>MER 76</b>	68,390	$65,203 \pm 1524$	2	2233	$+\!\!\!\!+\!\!\!\!\!+$	4	2040	#	10	2787		m	36,354	+	_
MER 83	26,390	$28,000 \pm 655$	9	462	+	5	1140	$1284 \pm 6$	12	1143	$1331 \pm 83$	15	38,097	+	0
<b>MER</b> 96	48,510	$48,745 \pm 1968$	0	1540	$^{\rm H}$	4	1800	+	6	2287	$2161 \pm 51$	9	37,765	$^{\rm H}$	-
MER 99	61,600	$60,838 \pm 1003$	-	2156	$^{\rm H}$	13	1620	+	11	2501	$2392 \pm 58$	4	37,350	$^{\rm H}$	0
MER 105	006'09	$60,357 \pm 2201$	-	2541	$^{\rm H}$	6	2640	+	0	3073	$2711 \pm 211$	12	38,014	$36,977 \pm 1718$	33
MER 112		$39,668 \pm 1802$			$+\!\!\!\!+\!\!\!\!\!+$			$2181 \pm 108$			$2628 \pm 86$			$^{\rm H}$	
MER 115	58,520	$61,374 \pm 1505$	5	1925	$^{\rm H}$	6	1980	$^{\rm H}$	4	2787	$2683 \pm 50$	4	37,765	$37,907 \pm 803$	0
MER 117	58,940	$689 \mp 609'09$	3	2002	$2015 \pm 33$	-	2100	$1951 \pm 31$	7	2787	$2758 \pm 92$	-	38,180		7
MER 119	57,820	$60,160 \pm 84$	4	2002	$^{+}$	0	1860	$1882 \pm 17$	_	2715	$2688 \pm 73$	_	37,599	$37,143 \pm 58$	-
Mean			33			7			2			7			2

\* Note that the percent difference for Sr is inflated due to its low concentrations in the obsidians. Horwitz et al. (1980) describe how, for any analytical technique, measurement uncertainties increase as concentrations decrease.

**Table 7**Comparison of ICP-MS data from Brown et al. (2013) to fully calibrated pXRF data for Merrick obsidian specimens not included in the calibration's linear regression analysis.

	Nb			Zr			Sr			Rb		
	ICP-MS	pXRF (cal)	%Diff	ICP-MS	pXRF (cal)	%Diff	ICP-MS	pXRF (cal)	%Diff*	ICP-MS	pXRF (cal)	%Diff
MER 34	288	271 ± 14	6	1290	1292 ± 62	0	7	7 11 ± 4	49	428	408 ± 21	5
MER 38	233	$213 \pm 7$	9	875	$799 \pm 31$	9	1	$3\pm1$	71	200	$180 \pm 5$	10
MER 45	253	$254\pm11$	1	1396	$1394 \pm 53$	0	5	$7 \pm 1$	31	212	$217 \pm 8$	3
MER 69	236	$234 \pm 2$	1	835	$1015 \pm 5$	19	43	$58 \pm 1$	31	246	$233 \pm 1$	5
MER 70	394	$409 \pm 7$	4	2628	$2605 \pm 45$	1	8	$11 \pm 1$	29	424	$429 \pm 10$	1
MER 75	260	$271 \pm 2$	4	1275	$1346 \pm 1$	5	3	$6 \pm 1$	77	202	$211 \pm 2$	4
MER 76	273	$282 \pm 4$	3	1328	$1361 \pm 13$	2	6	$9 \pm 1$	40	221	$218 \pm 3$	1
MER 83	298	$308 \pm 5$	3	1533	$1454 \pm 24$	5	4	$7 \pm 1$	56	452	$456 \pm 4$	1
MER 96	209	$222 \pm 6$	6	1390	$1374\pm42$	1	3	$3\pm1$	31	268	$272 \pm 9$	2
MER 99	250	$238 \pm 6$	5	1226	$1131 \pm 20$	8	7	$9 \pm 1$	24	274	$256 \pm 5$	7
MER 105	233	$260 \pm 7$	11	1201	$1408 \pm 47$	16	4	$6 \pm 1$	39	188	$217 \pm 9$	14
MER 112	493	$493 \pm 17$	0	3125	$3019 \pm 101$	3	8	$11 \pm 1$	24	393	$399 \pm 16$	2
MER 115	295	$305 \pm 8$	3	1533	$1530 \pm 30$	0	10	$13 \pm 1$	28	231	$242 \pm 9$	5
MER 117	292	$305 \pm 5$	4	1478	$1523\pm20$	3	9	$14 \pm 1$	37	229	$237 \pm 2$	4
MER 119	248	$299 \pm 3$	18	1163	$1491 \pm 12$	25	8	$14 \pm 1$	54	202	$231 \pm 2$	14
Mean			5			7			41			5
	Zn			Mn			Ti			Ca		
	ICP-MS	pXRF (cal)	%Diff	ICP-MS	pXRF (cal)	%Diff	ICP-MS	pXRF (cal)	%Diff	ICP-MS	pXRF (cal)	%Diff
MER 34	298	293 ± 20	2	458	413 ± 47	10	1116	1218 ± 66	9	1648	1989 ± 166	19
MER 38	347	$322 \pm 11$	7	3177	$2815 \pm 90$	12	4122	$3872 \pm 192$	6	7551	$6397 \pm 269$	17
MER 45	458	$469 \pm 21$	3	2093	$2103 \pm 127$	0	2324	$2315 \pm 61$	0	2892	$2950 \pm 146$	2
MER 69	163	$162 \pm 5$	1	1063	$996 \pm 16$	6	2904	$2865 \pm 61$	1	4828	$5687 \pm 561$	16
MER 70	532	$541 \pm 21$	2	1539	$1650 \pm 60$	7	1717	$1562 \pm 30$	9	2055	$2383 \pm 75$	15
MER 75	502	$517\pm8$	3	2064	$2231 \pm 26$	8	1574	$1607 \pm 69$	2	2852	$2911 \pm 20$	2
MER 76	480	$480 \pm 8$	0	1946	$2000 \pm 56$	3	1683	$1679 \pm 66$	0	2748	$2928 \pm 120$	6
MER 83	304	$330\pm8$	8	459	$471 \pm 38$	3	1025	$1152 \pm 6$	12	546	$1697 \pm 74$	103
MER 96	370	$378\pm24$	2	1338	$1391 \pm 59$	4	1744	$1792\pm34$	3	2275	$2442 \pm 46$	7
MER 99	457	$431 \pm 14$	6	1947	$1776 \pm 38$	9	1710	$1642 \pm 44$	4	2654	$2649 \pm 52$	0
MER 105	412	$453 \pm 13$	9	1940	$2162 \pm 103$	11	2213	$2401 \pm 86$	8	2641	$2936 \pm 189$	11
MER 112	382	$380 \pm 20$	0	1300	$1392\pm78$	7	2152	$1984 \pm 100$	8	2488	$2861\pm77$	14
MER 115	436	$469 \pm 3$	7	1823	$1973 \pm 116$	8	1751	$1728\pm10$	1	2083	$2911 \pm 45$	33
MER 117	444	$462 \pm 11$	4	1787	$1887 \pm 31$	5	1735	$1771 \pm 28$	2	2356	$2978 \pm 83$	23
					1001 : 00			1707   16	4.0	21.42	2016 . 65	2.1
MER 119	383	$457 \pm 17$	18	1548	$1884 \pm 26$	20	1499	$1707 \pm 16$	13	2142	$2916 \pm 65$	31

<sup>\*</sup> Percent difference for Sr is inflated due to its low concentrations. Horwitz et al. (1980) describe how, for any analytical technique, measurement uncertainties increase as concentration decreases.

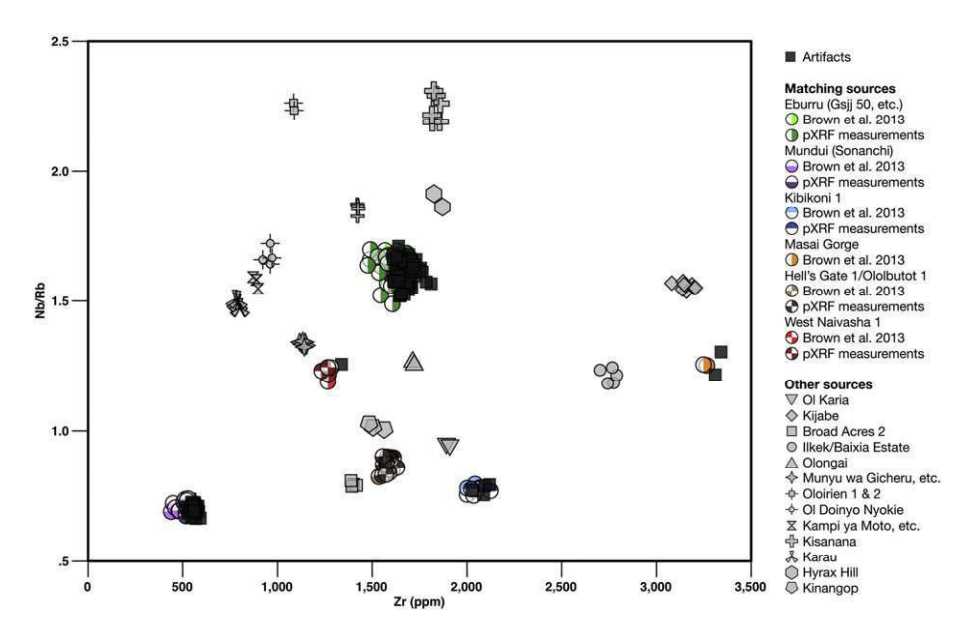


**Fig. 6.** Scatterplot of Zr versus Nb/Rb for the artifacts (black squares), their six matching geological sources (colorful circles), and select other obsidian sources reported by Brown et al. (2013) without matching artifacts (various grey symbols). For the identified sources, the published WDXRF data from Brown et al. (2013) are the lighter shades (e.g., light green for Eburru), while our calibrated pXRF data on geological specimens (when available) are the darker shades (e.g., dark green for Eburru). These measurements are available in Table 8.

 Table 8

 Our pXRF measurements of the 78 obsidian artifacts and their matching geological specimens as well as matching published WDXRF/EMPA data from Brown et al. (2013).

*										
Source	Site	Specimen/Artifact	Zr (ppm)	Nb (ppm)	Rb (ppm)	Nb/Rb	Sr (ppm)	Fe (ppm)	Mn (ppm)	Notes
Eburu GsJj 50, N slope, etc.		WDXRF/EMPA data from Brown et al. 2013	n et al. 2013							
		MER 100	1620	325	197	1.6	7	58380	2079	Brown et al. 2013 - Table 3, Naivasha-Nakuru
		MER 114	1646	327	208	1.6	12	29080	1925	Brown et al. 2013 - Table 3. Naivasha-Nakuru
		MFR 115	1613	330	190	1.7	! 4	58520	1925	Brown et al 2013 - Table 3 Naixasha-Naixu
		MED 116	1647	220	106	1.7	ר ע	20250	0200	Drown of al 2019 - Table 2, Ivalvasia-Ivanual
		MEN 110	104/	277	190	0 1	nı	38390	5002	BIOWII et al. 2013 - Table 3, Naivasiid-Ivakui u
		MEK II/	1589	316	061	I./	5	58940	7007	Brown et al. 2013 - Table 3, Naivasha-Nakuru
		MER 118	1623	319	196	1.6	6	2/960	7007	Brown et al. 2013 - Table 3, Naivasha-Nakuru
		MER 119	1598	317	190	1.7	∞	57820	2002	2013 - Table 3,
		MER 13	1641	329	198	1.7	_	59920	2002	2013 - Table 3,
		MER 25	1568	322	190	1.7	7	09209	1925	Brown et al. 2013 - Table 3, Naivasha-Nakuru
		MER 26	1582	315	188	1.7	~	09009	2079	Brown et al. 2013 - Table 3, Naivasha-Nakuru
		MER 72	1679	327	205	1.6	6	28660	2002	Brown et al. 2013 - Table 3, Naivasha-Nakuru
		MER 73	1637	325	196	1.7	8	58450	2079	Brown et al. 2013 - Table 3, Naivasha-Nakuru
		pXRF of Brown et al. 2013 geological	ogical reference specimens	ecimens						
		MER 115	1651	330	198	1.7	11	58839	2097	
		MER 115	1644	329	202	1.6	11	58887	2011	
		MER 115	1699	344	212	1.6	12	61360	2255	
		MER 117	1680	336	199	1.7	13	58908	2039	
		MER 117	1669	339	202	1.7	13	59858	1994	
		MER 117	1632	326	200	1.6	=	58331	1993	
		MER 119	1631	330	197	1.7	13	58618	2032	
		MER 119	1634	329	194	1.7	12	58521	2049	
		MER 119	1613	324	194	1.7	11	58459	1994	
		pXRF of other geological reference sp	nce specimens							
		ke01mr1a	1630	337	211	1.6	7	73876	2161	Sampling locus KEB16 in Ren et al. 2006
		ke01mr1a	1522	312	190	1.6	. 10	64609	2109	Sampling locus KFB16 in Ren et al. 2006
		ke01mr1a	1587	378	210	1.6	<u>.</u>	76817	2279	Sampling locus KFB16 in Ren et al. 2006
		keomman la	1480	207	105	1.0	01	7,0017	6177 VCUC	Sampling locus NED10 III Nell et al. 2000
		ke011111110	1469	307	103		10	91909	2034	י ק
		keulmric	1544	313	206	c.I	Ξ,	/0623	2155	et al.
		ke01mr1c	1579	327	509	1.6	6	71154	2235	et al.
		ke01mr1c	1490	306	180	1.7	12	61920	2102	et al.
		ke02mr1a	1547	317	194	1.6	8	62071	2159	Sampling locus KEB17 in Ren et al. 2006
		ke02mr1a	1606	326	219	1.5	6	72182	2157	et al.
		ke02mr1c	1629	343	211	1.6	6	72292	2175	Sampling locus KEB17 in Ren et al. 2006
		ke02mr1c	1600	330	211	1.6	∞	71825	2155	Sampling locus KEB17 in Ren et al. 2006
		ke02mr1c	1531	315	188	1.7	8	09/09	2111	Sampling locus KEB17 in Ren et al. 2006
		ke.2009.1	1536	316	196	1.6	6	64540	2407	et al.
		ke:2009.1	1476	303	185	1.6	10	61868	2195	et al.
		ke.2009.2	1574	323	194	1.7	6	64191	2290	Sampling locus KEB17 in Ren et al. 2006
		ke.2009.2	1582	321	195	1.6	10	64048	2391	Ren et al.
		pXRF of archaeological artifacts	s							
	Abindu	abindu ab10 11	1670	336	204	1.6	13	58708	1952	
		abindu ab10 5	1693	337	211	1.6	13	61255	1931	
		abindu ab11 064 10	1666	339	211	1.6	11	65695	1885	
		abindu ab11 15	1633	336	215	1.6	12	61859	1820	
		abindu ab3 12	1677	343	219	1.6	11	65250	1961	
		abindu ab6 6	1695	338	205	1.6	13	60194	1890	
		abindu ab9 13	1700	342	218	1.6	11	64141	1911	
	Agoro	agoro ag44! 3	1679	337	216	1.6	11	65470	1982	
	Jawuoyo	jawuoyo ja21 13	1697	341	207	1.6	13	61320	1988	
		jawuoyo ja26 5	1659	333	200	1.7	10	58839	1845	
		jawuoyo ja4 1	1664	332	202	1.6	11	58988	1960	
		Jawuoyo ja4 3	1752	352	216	1.6	14	62642	1981	
		jawuoyo ja43 16 a4300	1725	347	217	1.6	14	60644	1783	
		jawuoyo ja49 12	1568	338	216	1.6	Ι,	2/5/7	1720	
		Jawuoyo Jao/! 13	1504	327	200	1.0	41 o	71468	1986	
	Randhore	Jawuoyo Jao 4 randhore rd2 2	1510	327	192	1.0	12	7.1400	1928	
	Mailtailoic	randhore rd2 5	1807	356	201	1.7	14	65958	2123	
		ומותווסו בחק כ	1001	2	, , , ,	2	Ţ		7777	

	Brown et al. 2013 - Table 3, Naivasha-Nakuru Brown et al. 2013 - Table 3, Naivasha-Nakuru Brown et al. 2013 - Table 9, Naivasha-Nakuru Brown et al. 2013 - Table 3, Naivasha-Nakuru Brown et al. 2013 - Table 3, Naivasha-Nakuru	Brown et al. 2013 - Table 3, Naivasha-Nakuru Brown et al. 2013 - Table 3, Naivasha-Nakuru Brown et al. 2013 - Table 3, Naivasha-Nakuru Brown et al. 2013 - Table 5, Naivasha-Nakuru Brown et al. 2013 - Table 3, Naivasha-Nakuru Brown et al. 2013 - Table 3, Naivasha-Nakuru	Brown et al. 2013 - Table 3, Naivasha-Nakuru Brown et al. 2013 - Table 3, Naivasha-Nakuru
2042 2000 1861 1881 1853 1954 1955 1959 1909 1892 1977 2009 1805 1733 1733 1727 1904	462 539 462 462 462 502 390 491 485 471 474 470 523	385 385 385 385 385 385 312 301	297 1848 1771 1923 1729
67060 64145 66145 65139 65460 62038 62542 63284 62045 57772 56686 59789 58341 58802 62141 60957 62052 63293 61431	29400 27440 29400 26950 26390 26390 26284 27304 29327 26366 27323 30402 30560 29755 277044	2670 2670 26850 26850 26880 26880 2880 2880 29467 27973	27408 57330 56490 55058 60016
5 - 5 - 5 - 5 - 5 - 5 - 5 - 5 - 5 - 5 -		N	2 4 4 7 2 1 2 2 1 2 1 2 1 2 1 2 1 2 1 2 1 2 1
1.6 1.7 1.7 1.5 1.6 1.6 1.7 1.7 1.7 1.7 1.7 1.6 1.6 1.6 1.6 1.6 1.6 1.6 1.6 1.7 1.7 1.7 1.7 1.6 1.6 1.6 1.6 1.6 1.6 1.6 1.6 1.6 1.6	6.0 8.0 8.0 9.0 9.0 9.0 9.0 9.0 9.0 9.0 9.0 9.0 9	6 8 8 8 8 8 8 8 8 8 8 8 8 8 8 8 8 8 8 8	0.8 1.3 1.3 1.2
224 216 208 216 215 219 211 220 200 204 203 204 204 203 204 204 207 207 208 208 215 211 215 215 216 217 218 218 207 208 208 207 208 208 208 208 208 208 208 208 208 208	395 394 392 391 388 379 376 379 401 401 402 404 377	400 412 419 402 418 418 445 428	431 401 402 411 442
349 344 343 344 329 333 333 334 337 337 337 337 338 338 338 338	343 331 333 339 319 319 319 340 340 338 338 338 332 332 332 332	302 327 327 313 314 318 343 332 334	343 502 505 536 536
1705 1654 1659 1689 1689 1629 1629 1629 1621 1657 1660 1660 1660 1661 1661 1661 167 167 167 167 167 167	1573 1573 1607 1562 1613 1613 1632 1636 1596 1596 1596 1596 1576 1577	2000 2043 2000 2043 2066 2002 2051 2051 2051 2022 2022	
randhore rd2 7 1705 randhore rd27 12 165-5 randhore rd207 16 164-7 randhore rd207 16 168-7 randhore rd3 3 168-7 randhore rd3 9 168-7 randhore rd4 1 161-7 rangong rg10 1 161-7 rangong rg10 1 162-7 rangong rg10 4 162-7 rangong rg2 9 1620-7 rangong rg2 9 1620-7 rangong rg2 1 1 162-7 rangong rg2 1 1 162-7 rangong rg2 1 1 166-7 rangong rg3 5 1 166-7 rangong rg3 5 1 166-7 rangong rg3 1 1 167-7 rangong rg3 2 1 166-7 rangong rg3 1 1 167-7 rangong rg3 1 1 1 1 1 1 1 1 1 1 1 1 1 1 1 1 1 1 1	K80-399W 1596 MER 29 1577 MER 31 1607 MER 83 1552 MER 83 1553 pXRF of Brown et al. 2013 geological 1 MER 31 1613 MER 31 1639 MER 31 1639 MER 31 1596 MER 82 1558 MER 82 1556	MUNDSHEMPA data from Brown et al. CMN 24 MER 11 2006 MER 11 2004 MER 12 2005 MER 30 MER 30 MER 50 PXRF of other geological reference spe ke.2009.9 ke.2009.9 ke.2009.9 ke.2009.9 rangong 10 15 rangong 110 15	rangong rg29 6 2116 WDXRF/EMPA data from Brown et al. MER 90 3267 MER 91 3248 pXR of archaeological artifacts abindu ab10 063 2 3337 abindu ab10 2 3307
Rangong	D. C.	Rangong	Abindu
Hell's Gate 1/Ololbutot 1		Kibikoni 1	Masai Gorge Rockshelter Mundui (Sonanchi)

Table 8 (continued)

Notice											
100   100	Source	Site	Specimen/Artifact	Zr (ppm)	Nb (ppm)	Rb (ppm)	Nb/Rb	Sr (ppm)	Fe (ppm)	Mn (ppm)	Notes
Color   Colo			002 (Plc1)	439	200	290	0.7	9	14070	308	Brown et al. 2013 - Table 3. Naivasha-Nakuru
March   Marc			210b (Plc1)	450	207	287	0.7	i	14350	231	Brown et al. 2013 - Table 3. Naivasha-Nakuru
MRR 8 42 42 193 276 07 5 14210  MRR 8 462 472 193 278 07 5 14210  MRR 9 462 472 193 278 07 5 14210  MRR 9 462 472 193 278 07 5 1562  MRR 9 462 472 193 278 07 5 1562  MRR 9 462 472 193 278 07 5 1562  MRR 9 462 472 193 278 07 5 1562  MRR 9 462 472 193 278 07 5 1562  MRR 9 462 472 193 278 07 5 1562  MRR 9 462 472 193 278 07 5 1562  MRR 9 462 472 193 278 07 5 1562  MRR 9 100 100 100 100 100 100 100 100 100 1			CMN 12	461	188	267	0.7	3	13720	308	Brown et al. 2013 - Table 3, Naivasha-Nakuru
Milk of the geological reference specimens   194   281   07   5   11555     Milk of print geological reference specimens   194   281   07   5   11555     Milk of benefit   252   194   288   07   5   11555     Milk of benefit   252   194   288   07   5   11555     Milk of benefit   252   194   288   07   5   11555     Milk of benefit   252   194   288   07   5   11558     Milk of benefit   252   194   288   07   5   11558     Milk of benefit   252   194   288   07   5   11558     Milk of benefit   252   194   288   07   5   11558     Milk of benefit   252   194   288   07   5   11558     Milk of benefit   252   194   288   07   5   11558     Milk of benefit   252   194   288   07   5   11558     Milk of benefit   252   194   288   07   5   11558     Milk of benefit   252   194   284   07   5   11558     Milk of benefit   252   194   284   07   5   11558     Milk of benefit   254   294   294   07   5   11558     Milk of benefit   254   294   294   07   5   11558     Milk of benefit   254   294   294   07   5   11558     Milk of benefit   254   294   294   07   5   11558     Milk of benefit   254   294   294   07   5   11558     Milk of benefit   254   294   294   07   5   11558     Milk of benefit   254   294   294   294   294   294   294     Milk of benefit   254   294   294   294   294   294   294     Milk of benefit   254   294   294   294   294   294   294     Milk of benefit   254   294   294   294   294   294   294     Milk of benefit   254   294   294   294   294   294   294     Milk of benefit   254   294   294   294   294   294   294     Milk of benefit   254   294   294   294   294   294   294     Milk of benefit   254   294   294   294   294   294   294   294     Milk of benefit   254   294   294   294   294   294   294     Milk of benefit   254   294   294   294   294   294   294     Milk of benefit   254   294   294   294   294   294   294   294     Milk of benefit   254   294			MFR 7	478	191	276	0.7	. 00	14210	308	Brown et al. 2013 - Table 3. Naivasha-Nakum
Mainting protection of the p			MFR 8	482	193	278	0.7	יי ני	13650	385	Brown et al. 2013 - Table 3 Naivasha-Nakuru
Independent			pXRF of other geological refer	ence specimens		o i	3	,			
Red-Mart   S28   195   286   07   5   14077			ke04mr1a	520	194	281	0.7	4	15368		Sampling locus KO5 in Ren et al. 2006
Rechart   Rechart   STA   1947   286   07   5   15657			ke04mr1a	526	195	269	0.7	5	14077		Sampling locus KO5 in Ren et al. 2006
RedMart1   S22   194   286   07   4   1875			ke04mr1b	528	197	286	0.7	3	15637		Sampling locus KO5 in Ren et al. 2006
Red-Marrie         532         294         286         07         4         15828           Red-Marrie         532         195         286         07         5         1508           ReaDOB4         538         195         286         07         5         14085           ReaDOB4         538         192         282         07         4         15174           ReaDOB4         535         193         262         07         4         1574           ReaDOB4         535         194         284         07         5         14085           ReaDOB4         535         194         284         07         4         1574           ReaDOB4         535         194         284         07         4         1574           ReaDOB4         517         191         284         07         4         1586           ReaDOB4         517         194         279         07         4         1586           ReaDOB4         517         191         279         07         4         1586           ReaDOB4         517         519         279         07         4         1586           <			ke04mr1b	527	193	265	0.7	5	13679		Sampling locus KO5 in Ren et al. 2006
RecObserved         532         195         286         0.7         4         15317           RecOLOGA         513         192         262         0.7         5         14082           RecOLOGAS         513         192         262         0.7         5         14082           RecOLOGAS         512         193         262         0.7         4         13744           RecOLOGAS         512         193         263         0.7         4         13745           RecOLOGAS         517         191         284         0.7         4         13785           RecOLOGAS         517         191         284         0.7         4         13785           Abrida         abrida abil 19         547         191         284         0.7         4         13785           Abrida abil 17         532         194         279         0.7         4         13785           Abrida abil 17         547         191         284         0.7         4         13785           Abrida abil 18         547         194         275         0.7         4         13785           Abrida abilida			ke04mr1c	532	204	298	0.7	4	15828		Sampling locus KO5 in Ren et al. 2006
Re. 20064   513   195   265   197   55   14085   140			ke04mr1c	532	195	286	0.7	4	15317		Sampling locus KO5 in Ren et al. 2006
Proceedings			ke 2009.4	528	195	263	0.7	. 17.	14085	295	Sampling locus KO5 in Ren et al. 2006
Part			ke 2009 4	513	192	292	0.7	, r.	13537	288	Sampling locus KO5 in Ren et al. 2006
Abindu abintu abid abid abid abid abid abid abid abid			NC:2003:4	515	102	202	0.7	) <b>-</b>	12744	200	Samping rocus NOS III NCII et al. 2000
Abindu aborto da 1815 1818 274 077 4 14500  Abindu ab 181 9 547 191 284 077 4 14500  Abindu ab 181 9 547 191 284 077 4 1588  Abundu ab 181 9 547 191 284 077 4 1588  Abundu ab 181 9 547 191 284 077 4 1588  Abundu ab 181 9 547 191 284 077 4 1588  Abundu ab 181 9 547 191 284 077 184 1888  Abundu ab 181 9 547 191 284 077 184 1888  Abundu ab 181 9 547 191 284 077 184 1888  Abundu ab 181 9 547 191 284 077 184 1888  Abundu ab 181 9 547 191 184 075 184 077 184 1888  Abundu ab 181 9 547 191 184 075 184 1888  Abundu ab 181 9 547 191 184 075 184 1888  Abundu ab 181 9 547 191 184 075 184 1888  Abundu ab 181 9 547 184 184 184 184 184 184 184 184 184 184			ke.2003.8 ka 3009.8	522	192	623 263	0.7	<b>4</b> <	13683	200	
Abindu			Ne.2009.6	322 515	189	202	0.7	<b>1</b> ~	14070	105	
Abindu ab			Ke:2009.8	515	101	4/7 197	0.7	4 п	15787	163	
Abindu abindu abi 1 52 154 156 273 0.7 4 1 13500  Abindu abi 10 7 52 184 255 0.7 8 1 15867  abindu abi 11 552 184 255 0.7 8 1 15867  abindu abi 12 522 184 255 0.7 8 1 15867  abindu abi 12 522 184 255 0.7 8 1 15867  abindu abi 12 522 184 255 0.7 8 1 15867  abindu abi 12 522 184 255 0.7 8 1 15867  abindu abi 12 522 184 255 0.7 8 1 15867  abindu abi 12 522 184 255 0.7 8 1 15867  abindu abi 12 522 184 255 0.7 8 1 15867  abindu abi 12 522 184 255 0.7 8 1 15867  abindu abi 12 522 184 254 0.7 8 1 15867  bi awuoyo jac 1 1 4276 554 199 284 0.7 5 1 15861  jawuoyo jac 1 1 4276 554 199 284 0.7 5 1 15861  jawuoyo jac 1 1 4276 555 199 284 0.7 7 7 1 17697  jawuoyo jac 1 1 4276 54 199 284 0.7 7 7 1 17697  jawuoyo jac 1 1 4276 54 199 284 0.7 7 7 1 17697  jawuoyo jac 1 1 4276 54 199 284 0.7 7 7 1 17697  jawuoyo jac 1 1 4276 54 199 284 0.7 7 7 1 17697  kangong tandhore rd 14 54 54 199 284 0.7 7 7 1 16987  kangong tandhore rd 14 54 54 199 27 2 2 2 2 2 2 2 2 2 2 2 2 2 2 2 2 2			KE.Z009.8	517	191	487 027	0.7	0 4	15283	308	
Abindu abindu abit         Abindu abindu abit         547         196         273         0.7         4         1896           abindu abit         547         191         284         0.7         4         1994           abindu abit         547         191         285         0.7         4         1589           abindu abit         552         195         274         0.7         5         1589           abindu abit         560         199         274         0.7         4         1589           abindu abit         560         199         274         0.7         4         1589           abindu abit         560         199         274         0.7         4         1589           abindu abit         560         199         284         0.7         5         1581           jawunojo jaz         11 aking         275         199         283         0.7         5         1480           jawunojo jaz         57         20         284         194         284         1750         1480           jawunojo jaz         57         20         282         20         2         11408           jawunojo jaz <t< th=""><th></th><th></th><th>RE.ZUU9.8</th><th></th><th>194</th><th>6/7</th><th>٥.٧</th><th>4</th><th>13380</th><th>797</th><th></th></t<>			RE.ZUU9.8		194	6/7	٥.٧	4	13380	797	
Agoro abindu abil 9 547 1916 264 07, 5 19408  Agoro agoro ago 2 1,2 552 195 283 07 4 11385  Agoro agoro ago 2 2,2 50 199 254 07 5 11387  Agoro agoro ago 2 2,2 59 192 259 07 5 113815  Agoro agoro ago 2 2,2 59 192 259 07 5 113815  Agoro agoro ago 2 2,2 59 192 259 07 5 113815  Agoro agoro ago 2 2,2 59 192 259 07 5 113815  Jawunoyo jazo 11 2 2 2 2 2 2 2 2 2 2 2 2 2 2 2 2 2 2			pake of archdeological artifac		0	1	1	ı	0000		
Agaro agon agon agon agon agon agon agon ago		Abındu	abindu ab? 4	561	196	2/3	0.7	ς.	14908	86	
Agron a plind to 40.7 1 53.2 159 255 0.7 8 4 15380  Agron a plind to 40.7 1 53.2 159 259 0.7 8 4 15380  Agron a part a 20.2 15.5 29 5.6 199 2.7 5 0.7 8 1 15381  Agron a part a 20.2 15.5 29 5.6 199 2.7 0.7 5 1 15381  Jawuoyo ja20.1 1 a 27.6 564 199 283 0.7 5 6 113408  Jawuoyo ja20.1 1 a 23.5 1195 288 0.7 7 5 115831  Jawuoyo ja20.1 1 a 23.5 1195 288 0.7 7 5 115831  Jawuoyo ja20 1 2.5 29 2.7 0.7 5 115831  Jawuoyo ja60 1 a 22.9 5.7 5 201 287 0.7 5 115831  Jawuoyo ja60 1 a 22.9 5.7 5 201 287 0.7 5 115831  Jawuoyo ja60 1 a 22.9 5.7 5 201 287 0.7 5 115831  Jawuoyo ja60 1 a 22.9 5.7 5 201 287 0.7 5 115831  Jawuoyo ja60 1 a 22.9 5.7 5 201 287 0.7 5 115831  Jawuoyo ja60 1 a 22.9 5.7 5 201 287 0.7 5 115831  Jawuoyo ja60 1 a 22.9 5.7 5 201 287 0.7 5 115831  Jawuoyo ja60 1 a 22.9 5.7 5 201 287 0.7 5 115831  Jawuoyo ja60 1 a 22.9 5.7 5 201 287 0.7 5 115831  Jawuoyo ja60 1 a 22.9 5.7 5 201 287 0.7 5 115831  Jawuoyo ja60 1 a 22.9 5.7 5 201 287 0.7 5 115831  Jawuoyo ja60 1 a 22.9 5.7 5 201 287 0.7 5 115831  Jawuoyo ja60 1 a 22.9 5.7 5 201 288 0.7 5 115831  Jawuoyo ja60 1 a 22.9 5.7 5 202 289 0.7 5 115831  Jawuoyo ja60 1 a 22.9 5.7 5 202 289 0.7 5 115831  Jawuoyo ja60 1 a 22.9 5.7 5 202 289 0.7 5 115831  Jawuoyo ja60 1 a 22.0 5 202 289 0.7 5 6 115831  Jawuoyo ja60 1 a 22.0 5 202 289 0.7 6 6 115831  Jawuoyo ja60 1 a 20.1 5			abindu abi i 9	747	191	264	0.7	4.	13949	160	
Agoro agon agon agon agon agon agon agon ago			abindu abiz i	797	195	783	0.7	4 (	1586/	18/	
Agono			abindu ab177	532	184	255	0.7	»	15299		
Agono agono 24 14 515 192 259 07 4 13385  Agono agono 25 25 25 29 8 20 0 7 5 13381  Agono agono 25 25 25 25 25 25 25 25 25 25 25 25 25			abindu ab/ 8	560	199	2/4	0.7	ς,	14859		
Agono         agono ag207 1         18.3         2.2         0.7         2         13313           Jawuoyo         agono ag207 1         42.5         19.9         224         0.7         5         15313           Jawuoyo         jawuoyo ja20 1         14.475         564         19.9         28.3         0.7         5         15318           jawuoyo ja20 1         355         195         287         0.7         3         14642           jawuoyo ja20 1         453         195         287         0.7         5         13481           jawuoyo ja60 10 a4299         577         201         284         0.7         7         14642           jawuoyo ja60 10 a4299         577         201         284         0.7         7         17891           jawuoyo ja60 10 a4299         577         201         284         0.7         7         17892           jawuoyo ja60 10 a4299         577         201         284         0.7         7         17892           jawuoyo ja60 10 a4299         577         201         284         0.7         7         17892           jawuoyo ja60 10 a4299         577         201         284         0.7         4         <			abindu ab9 023 14	535	192	259	0.7	4 (	13385	0	
Jawnoyo   Jawn		Agoro	agoro ag26 2 a5299	510	183	252	0.7	2	13313	226	
Jawnoyo ja37 8   Jawnoyo ja36 10 a 239   Jawnoyo j			agoro ag29? 1	280	204	294	0.7	2	15831	107	
Jawnoyo jad 3 1 4 555   195   268   0.7 5 5 1 14642     Jawnoyo jad 2		Jawuoyo	jawuoyo ja26 11 a4276	564	199	283	0.7	9	13408		
Nyaidha         Jawuoyo ja62         535         195         273         0.7         3         14168           jawuoyo ja60         534         195         254         0.7         5         15891           jawuoyo ja60         517         186         254         0.7         7         7         17607           jawuoyo ja60         548         190         265         0.7         5         13962           jawuoyo ja60         548         194         284         0.7         7         17607           jawuoyo ja60         577         201         281         0.7         5         15582           jawuoyo ja60         577         201         284         0.7         7         17607           jawuoyo ja60         577         201         284         0.7         7         17599           jawuoyo ja60         577         204         284         0.7         7         17799           jawuoyo ja60         577         204         284         0.7         7         17799           jawuoyo ja60         577         204         204         295         0.7         4         15194           jawuoyo ja60         578			jawuoyo ja37 8	555	195	268	0.7	2	14642	156	
Jawuoyo Ja60 1 24299 517 201 285 0.7 5 13891  Jawuoyo Ja60 1 24299 517 186 246 0.7 5 12020  Jawuoyo Ja60 1 24299 517 186 246 0.7 5 12020  Jawuoyo Ja60 1 24299 517 201 214 0.7 5 12020  Jawuoyo Ja60 1 2429 210 210 214 0.7 5 12020  Jawuoyo Ja60 1 2429 210 214 0.7 5 12020  Randhore radahore rad 1 2 543 194 284 0.7 7 1779  Randhore radahore rad 1 5 564 204 224 0.7 7 1779  Rangong radahore rad 1 5 554 200 205 286 0.7 5 15887  Rangong radahore rad 1 10 557 200 289 0.7 10 16944  randhore rad 1 10 557 200 289 0.7 10 16944  randhore rad 1 11 537 202 284 0.7 5 15682  randhore rad 1 11 537 202 284 0.7 10 16944  randhore rad 1 11 537 202 289 0.7 5 15682  randhore rad 1 11 550 199 275 0.7 5 15682  rangong rada 1 2 550 199 275 0.7 5 15688  rangong rada 2 1 2 550 205 289 0.7 5 15688  rangong rada 2 1 2 551 201 278 0.7 5 15688  rangong rada 2 1 2 551 201 278 0.7 5 15688  rangong rada 2 1 255 205 299 0.7 6 15944  MRR 99 1266 264 278 278 0.7 5 15848  WRR 99 1266 264 278 278 0.7 5 15688  Abindu abhotd abb 2 1282 278 284 288 289 289 289 289 289 289 289 289 289			jawuoyo ja43 14	535	195	273	0.7	ന	14168		
jawuoyo ja60 10 44299 517 186 254 0.7 4 12020 jawuoyo ja60 7 559 210 281 0.7 7 17607 jawuoyo ja86 548 193 265 0.7 5 13962 jawuoyo ja86 548 193 265 0.7 5 13962 jawuoyo ja86 548 194 281 0.7 7 17607 jawuoyo ja8 6 548 194 281 0.7 7 17607 jawuoyo ja8 6 548 194 281 0.7 7 17609 Randhore rd 14 542 194 281 0.7 7 17799 Randhore rd 21 5 560 205 205 0.7 6 15344 randhore rd 21 5 50 202 209 0.7 8 15343 randhore rd 21 7 550 200 209 0.7 8 15019 randhore rd 21 7 550 200 209 0.7 6 16494 randhore rd 21 8 550 202 289 0.7 10 16494 randhore rd 21 8 550 202 289 0.7 10 16494 randhore rd 21 550 199 277 0.7 7 14058 rangong rg 21 18 550 205 209 0.7 6 14668 rangong rg 21 18 550 205 209 0.7 6 15594 rangong rg 21 2 550 205 209 0.7 6 15594 rangong rg 21 2 550 205 209 0.7 6 15594 rangong rg 21 2 550 205 209 0.7 6 15594 rangong rg 21 2 550 205 209 0.7 6 15594 rangong rg 21 2 550 205 209 0.7 6 15594 rangong rg 21 2 550 205 209 0.7 6 15594 rangong rg 21 2 550 205 209 0.7 6 5 15694 rangong rg 21 2 550 205 209 0.7 6 5 15694 rangong rg 21 2 550 204 204 2.7 6 5 15694 rangong rg 21 2 550 204 204 2.7 6 5 15694 rangong rg 21 2 550 204 204 2.7 6 5 15694 rangong rg 21 2 550 204 204 2.7 6 5 15694 rangong rg 21 2 550 204 204 2.7 6 5 15694 rangong rg 21 2 550 204 204 2.7 6 5 15694 rangong rg 21 2 550 204 204 2.7 6 5 15694 rangong rg 21 2 550 204 204 2.7 6 5 15694 rangong rg 21 2 550 204 204 2.7 6 5 15694 rangong rg 21 2 550 204 204 2.7 6 5 15694 rangong rg 21 2 550 204 204 2.7 6			jawuoyo ja6 2	575	201	287	0.7	2	15891	124	
Jawnoyo jado 7			jawuoyo ja60 10 a4299	517	186	254	0.7	4 -	12020		
Nyaidha   nyaidha ny3   548   193   265   0.7   5   1582     Nyaidha   nyaidha ny3   543   194   284   0.7   7   1799     Randhore rd164   542   194   284   0.7   7   17799     Randhore rd164   542   194   284   0.7   7   17799     Randhore rd114   564   204   295   0.7   4   15943     randhore rd215   554   202   286   0.7   8   15887     randhore rd217   554   200   279   0.7   8   15887     randhore rd3 18   550   202   284   0.7   10   16494     randhore rd4 11   537   200   289   0.7   10   16494     randhore rd4 11   537   202   289   0.7   4   15997     randhore rd4 11   557   202   289   0.7   6   15897     randhore rd4 11   557   202   289   0.7   6   15897     randhore rd4 11   550   199   278   0.7   6   15897     randhore rd4 11   550   205   298   0.7   6   15897     randhore rd4 11   550   205   298   0.7   6   15897     randhore rd4 11   550   205   299   0.7   6   15894     randhore rd4 11   550   205   205   205   205   205   205   205     rangong rg2 3			jawuoyo ja60 7	589	210	314	0.7	7	17607	143	
Nyaidha         jawuoyo Jab 9         577         201         281         0.7         5         1582           Randhore         randhore rd 16 4         543         194         284         0.7         7         17799           Randhore rd 14         564         204         295         0.7         4         15144           randhore rd 15         560         202         286         0.7         4         15384           randhore rd 17         550         202         294         0.7         3         15019           randhore rd 11         557         202         294         0.7         3         15019           randhore rd 11         57         202         294         0.7         3         15019           randhore rd 11         57         202         289         0.7         4         1589           randhore rd 11         57         202         289         0.7         5         1599           randhore rd 21         55         199         275         0.7         6         1468           randhore rd 21         55         199         275         0.7         6         1468           randorg 22.18         54<			jawuoyo ja8 6	548	193	265	0.7	2	13962	!	
Myaddha         Hyaddha Hyaddha Hya         154         184         284         0.7         7         1779           Randhore         randhore rd2 14         542         194         281         0.7         4         15114           randhore rd2 14         560         205         286         0.7         4         15114           randhore rd2 15         560         205         286         0.7         4         1594           randhore rd2 17         554         200         289         0.7         4         1591           randhore rd4 10         567         200         289         0.7         4         1569           randhore rd4 11         537         202         289         0.7         4         1569           randhore rd4 11         537         202         289         0.7         4         1569           randhore rd4 11         537         202         289         0.7         4         1569           randhore rd4 11         537         202         289         0.7         4         1569           rangong rg2 14         54         201         277         0.7         6         14626           rangong rg2 14		:	jawuoyo ja9 9	577	201	281	0.7	ı cı	15582	119	
Randhore radio and formation radio of and proper radio of and thore radio of a section of and thore radio of a section of and thore radio of a section of		Nyaidha -	nyaidha ny3 1	543	194	284	0.7	,	17/99		
randhore rd214 564 204 225 0.7 4 15943 randhore rd217 556 205 286 0.7 5 15384 randhore rd217 554 200 279 0.7 8 15887 randhore rd218 550 202 294 0.7 3 15019 randhore rd318 550 202 294 0.7 3 15019 randhore rd318 551 200 289 0.7 4 15692 randhore rd318 553 196 288 0.7 5 1694 randhore rd318 553 199 275 0.7 6 14668 rangong rg10 21 550 199 275 0.7 6 14668 rangong rg21 4 554 198 278 0.7 6 15954 rangong rg21 5 555 205 299 0.7 6 15954 rangong rg20 0 551 201 279 0.7 6 15954 rangong rg20 0 551 201 279 0.7 6 15954 rangong rg20 10 551 201 279 0.7 6 15954 rangong rg20 10 551 201 279 0.7 6 6 15954 rangong rg20 10 551 201 279 0.7 6 6 15954 rangong rg20 10 551 201 279 0.7 6 6 15954 rangong rg20 10 551 201 279 0.7 6 6 15954 rangong rg20 10 551 201 279 0.7 6 6 15954 rangong rg20 10 551 201 279 0.7 6 6 15954 rangong rg20 10 551 201 279 0.7 6 6 15954 rangong rg20 10 551 201 279 0.7 6 6 15954 rangong rg20 10 551 201 201 279 0.7 6 6 15954 rangong rg20 10 551 205 295 0.7 6 6 15848 rangong rg20 10 551 205 295 0.7 6 6 15848 rangong rg20 10 551 205 295 0.7 6 6 15848 rangong rg20 10 551 205 295 0.7 6 6 15848 rangong rg20 10 551 205 295 0.7 6 6 15848 rangong rg20 10 551 205 295 0.7 6 6 15848 rangong rg20 10 551 205 295 0.7 6 6 15848 rangong rg20 10 551 205 295 0.7 6 6 15848 rangong rg20 10 551 205 295 0.7 6 6 15848 rangong rg20 10 551 205 295 0.7 6 6 15848 rangong rg20 10 551 205 295 0.7 6 6 15848 rangong rg20 1269 264 217 1.2 8 58396 rangong rg20 10 50243 1335 284 226 13 8 61808		Randhore	randhore rd16 4	542	194	281	0.7	4 .	15114		
Rangong         rangong rg2 18         554         205         289         0.7         5         1584           randhore rd2 17         554         200         289         0.7         3         15887           randhore rd4 10         567         200         280         0.7         4         15694           randhore rd4 11         537         202         288         0.7         4         15692           randhore rd4 11         537         196         288         0.7         4         15692           randhore rd4 11         537         196         288         0.7         6         14668           randhore rd4 11         550         199         275         0.7         6         14668           randhore rd4 11         550         198         275         0.7         6         14678           rangong rg2 18         544         201         277         0.7         7         14978           rangong rg2 14         555         205         299         0.7         6         15848           WXXRFEWPA data from Brown et al. 2013 geological reference specimens         277         1.2         8         60347           MER 99         1269			randhore rd2 14	564	204	295	0.7	4 r	15943		
Rangong         Transporter of 12			randhono 142 15	360 FF4	203	027	0.7	n º	15007		
Rangong         Transporter (1)         500         202         254         0.7         10         16494           randhore r(4)         1         537         202         289         0.7         4         15694           randhore r(4)         1         537         202         289         0.7         4         15697           randhore r(4)         1         550         199         275         0.7         6         15697           rangong rg10 21         550         199         277         0.7         7         14668           rangong rg2 14         554         198         278         0.7         6         15954           rangong rg2 14         554         198         278         0.7         6         15954           rangong rg2 14         554         10         279         0.7         6         15954           rangong rg2 10         551         201         279         0.7         6         15954           WDXRF/EMPA data from Brown et al. 2013 geological reference specimens         222         1.2         3         61600           MER 99         1269         264         217         1.2         8         5396			randhoro rd2 18	550	200	907	0.7	0 6	15010		
Rangong         randhore rdd37 8         553         205         289         0.7         4.0         15692           Rangong         randhore rdd37 8         553         196         288         0.7         5         15692           randhore rdd37 8         554         199         275         0.7         6         15997           rangong rg23 18         544         201         277         0.7         7         14978           rangong rg21 4         554         198         278         0.7         5         15058           rangong rg21 4         551         201         279         0.7         6         15058           rangong rg9 10         551         201         279         0.7         6         15058           WDXRF/EMPA data from Brown et al. 2013 geological reference specimens         1266         264         222         1.2         3         61600           MER 99         1266         264         217         1.2         8         5396           MER 99         1269         269         216         1.2         8         5396           MER 99         1266         269         216         1.2         8         5396 <t< th=""><th></th><th></th><th>randhore rd4 10</th><th>567</th><th>207</th><th>280</th><th>0.7</th><th>n ⊊</th><th>16494</th><th>160</th><th></th></t<>			randhore rd4 10	567	207	280	0.7	n ⊊	16494	160	
Rangong         randthore rd637 8         553         196         288         0.7         5         1590           Rangong         rangong rg23 18         544         201         275         0.7         6         14668           rangong rg23 18         544         201         277         0.7         7         14978           rangong rg21 4         554         198         278         0.7         5         15058           rangong rg2 10         551         201         279         0.7         6         1558           rangong rg9 10         551         205         299         0.7         6         1568           rangong rg9 10         551         201         279         0.7         6         1568           WER 99         1266         264         222         1.2         3         6160           pXRF of Brown et al. 2013 geological reference specimens         264         217         1.2         8         60347           MER 99         1269         269         216         1.2         8         53956           MER 99         1266         269         216         1.2         8         58949           pXRF of archaeological art			randhore rd4 11	537	202	289	0.7	5 4	15692	3	
Rangong         rangong rg23 18         550         199         275         0.7         6         14668           rangong rg23 18         544         201         277         0.7         7         14978           rangong rg21 14         554         198         278         0.7         5         15058           rangong rg21 2         565         205         209         0.7         6         15054           rangong rg2 10         555         205         295         0.7         6         15848           WDXRF/EMPA data from Brown et al. 2013         1260         25         1.2         3         61600           MER 99         1269         1269         264         217         1.2         8         60347           MER 99         1269         1269         269         12         8         5936           MER 99         1260         269         216         1.2         8         5936           MER 99         1266         269         216         1.2         8         5936           Abindu ab9 0243         1335         284         26         1.3         8         61808			randhore rd63? 8	553	196	288	0.7	2	15997		
rangong rg23 18         544         201         277         0.7         7         14978           rangong rg25 14         554         198         278         0.7         5         15058           rangong rg2 10         565         205         299         0.7         6         15954           rangong rg2 10         551         201         299         0.7         5         14626           rangong rg2 10         555         205         295         0.7         6         15848           WIXKRFEMPA data from Brown et al. 2013         1266         264         222         1.2         3         61600           DKR 99         1269         264         217         1.2         8         59366           MER 99         1289         272         218         1.2         8         59366           MER 99         1266         269         216         1.2         8         59366           MER 99         1266         269         216         1.2         8         58949           pXRF of archaeological artifacts         135         284         286         1.3         8         61808		Rangong	rangong rg10 21	550	199	275	0.7	9	14668		
rangong rg25 14     554     198     278     0.7     5     15058       rangong rg6 12     565     205     299     0.7     6     15954       rangong rg2 10     551     201     279     0.7     5     14626       rangong rg9 23     555     205     295     0.7     6     15848       WDKRFIEMPA datar from Brown et al. 2013     1266     264     222     1.2     3     61600       DKRF 99     1269     264     217     1.2     8     60347       MER 99     1282     272     218     1.2     8     59396       MER 99     1266     269     216     1.2     8     58396       MER 99     1266     269     216     1.2     8     58394       Abindu ab9 024 3     1335     284     226     1.3     8     61808		)	rangong rg23 18	544	201	277	0.7	7	14978	118	
rangong rg6 12         565         205         299         0.7         6         15954           rangong rg9 10         551         201         279         0.7         5         14626           rangong rg9 23         555         205         295         0.7         5         15848           MCR 99         1266         264         222         1.2         3         61600           pXRF 99         1269         264         217         1.2         8         60347           MER 99         1289         128         217         1.2         8         59366           MER 99         1266         269         216         1.2         8         58949           PXRF of archaeological artifacts         1335         284         226         1.3         8         61808			rangong rg25 14	554	198	278	0.7	5	15058	173	
Tangong rg9 10 551 201 279 0.7 5 14626 Tangong rg9 23 555 205 295 0.7 6 15848  WDXRF/EMPA data from Brown et al. 2013 geological reference specimens  MER 99 1266 269 216 12 8 60347  MER 99 1266 269 216 12 8 5936  MER 99 1266 269 216 12 8 5936  Abindu ab9 024 3 1335 284 226 1.3 8 61808			rangong rg6 12	565	205	299	0.7	9	15954		
A rangong rg9 23 555 205 295 0.7 6 15848  WOXRFEMPA data from Brown et al. 2013  MER 99 1269 272 217 1.2 8 60347  MER 99 1266 269 216 1.2 8 69347  MER 99 1266 269 216 1.2 8 59396  MER 99 1268 269 216 1.2 8 59396  Abindu abb 024 3 1335 284 226 1.3 8 61808			rangong rg9 10	551	201	279	0.7	5	14626	107	
WDXRF/EMPA data from Brown et al. 2013     22     1.2     3     61600       MER 99     126     264     217     1.2     3     61600       MER 99     1282     272     217     1.2     8     60347       MER 99     1282     272     218     1.2     8     59396       MER 99     1266     269     216     1.2     8     58949       pXRF of archaeological artifacts     Abindu abb 024 3     1335     284     226     1.3     8     61808			rangong rg9 23	555	205	295	0.7	9	15848		
MER 99 1266 264 222 1.2 3 61600  PXRP of Brown et al. 2013 geological reference specimens  MER 99 1282 272 218 1.2 8 69347  MER 99 1266 269 216 1.2 8 58349  PXRP of archaeological artifacts  a bindu ab 9 024 3 1335 284 226 1.3 8 61808	West Naivasha 1		WDXRE/EMPA data from Brov	vn et al. 2013							
pXRF of Brown et al. 2013 geological reference specimens     1269     264     217     1.2     8     60347       MER 99     1282     272     218     1.2     8     59396       MER 99     1266     269     216     1.2     8     58949       pXRF of archaeological artifacts     abindu ab9 024 3     1335     284     226     1.3     8     61808			MER 99	1266	264	222	1.2	3	61600	2156	Brown et al. 2013 - Table 3, Naivasha-Nakuru
MER 99     1269     264     217     1.2     8     60347       MER 99     1282     272     218     1.2     8     5936       MER 99     1266     269     216     1.2     8     58949       pXRP of archaeological artifacts     abindu ab9 024 3     1335     284     226     1.3     8     61808			pXRF of Brown et al. 2013 gec	logical reference sp	ecimens						
MER 99 1282 272 218 1.2 8 59396 MER 99 1266 269 216 1.2 8 58949 pXRP of archaeological artifacts abindu ab9 024 3 1335 284 226 1.3 8 61808			MER 99	1269	264	217	1.2	∞ '	60347	1966	
MEK 99 1266 269 216 1.2 8 58949 pXRF of archaeological artifacts abindu ab9 024 3 1335 284 226 1.3 8 61808			MER 99	1282	272	218	1.2	∞ (	59396	1906	
pover of architectural arguments abindu abg 024 3 1335 284 226 1.3 8 61808			MER 99		697	716	1.2	×	58949	1903	
		Abindu	pxkr oj archaeologicai artijac abindu ab9 024 3		284	926	13	œ	61808	1954	
						01	3				

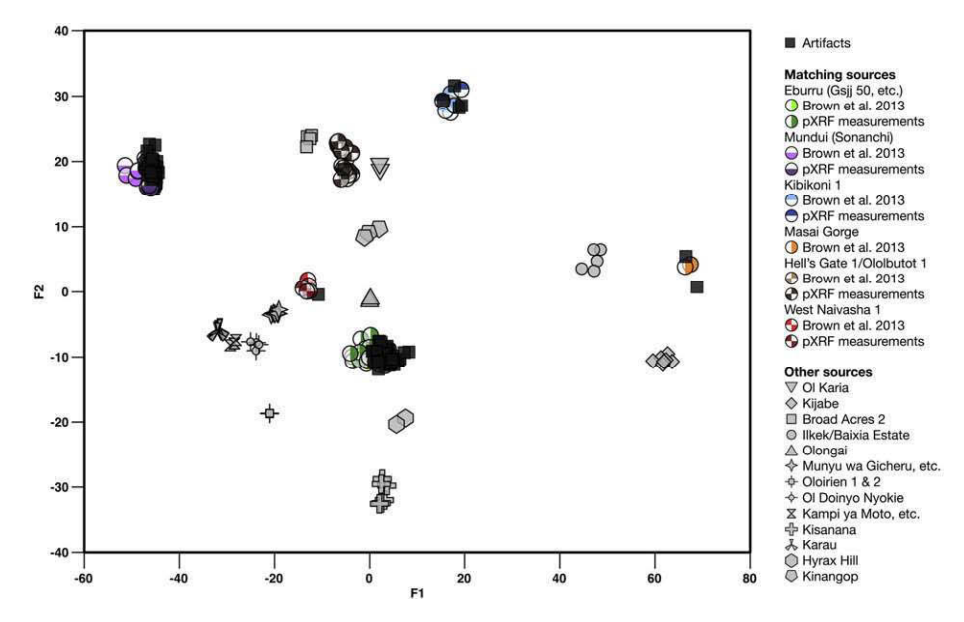
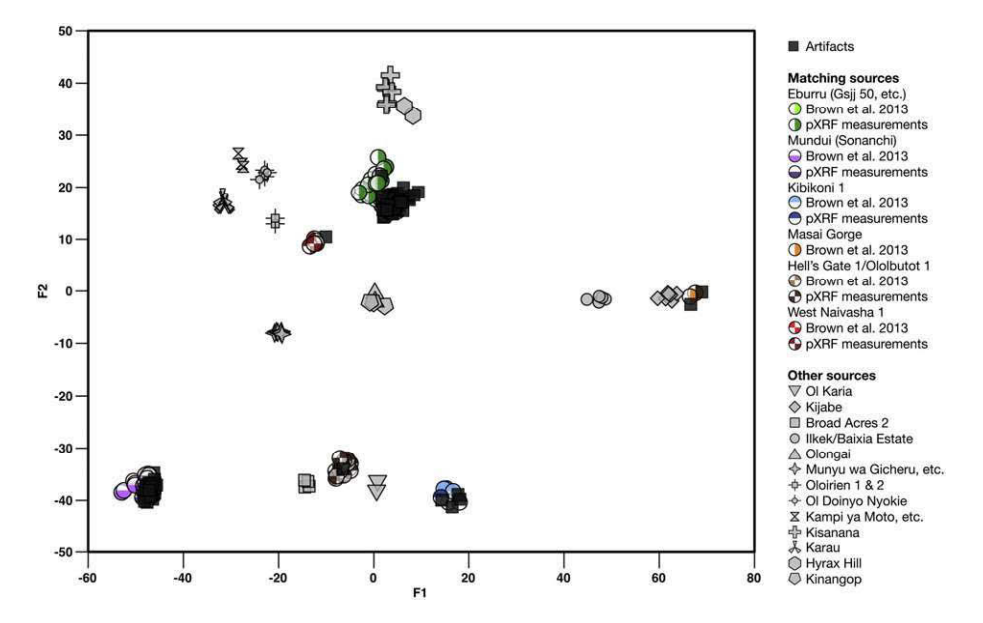


Fig. 7. Discriminant functions were derived with source as the grouping variable and Zr, Rb, Nb, and Sr as predicting variables. The resulting scatterplot shows the artifacts (black squares), their six matching geological sources (colorful circles), and select other obsidian sources reported by Brown et al. (2013) without matching artifacts (various grey symbols). Like Fig. 6, the published WDXRF data from Brown et al. (2013) are the lighter shades (e.g., light green for Eburru), while our calibrated pXRF data on geological specimens (when available) are the darker shades (e.g., dark green for Eburru).

sheetwash, and bedrock dissolution processes. They were excavated to depths of 0.75–3.0 m, and their deposits exhibited few stratigraphic distinctions and contained evidence for post-depositional disturbance (Gabel, 1969). Radiocarbon dates on charcoal run in the mid-1960s suggest ages of ~1.2–2.4 ka for the deposits (Gabel, 1969), but given that these samples consisted of aggregated pieces of charcoal tested more than four decades ago, these results should be treated with caution.

Gabel (1969) reported recent ceramics from each of the six rock shelters. Many of the ceramic styles that he described are consistent with what we now know to be Kansyore (ceramic LSA) wares (at Rangong and Abindu) and Urewe (Iron Age agropastoralist) wares (at Nyaidha) (Lane, 2004), although the Kansyore identification is questioned by some (Dale and Ashley, 2010). None of the ceramics are

clearly Elmenteitan or SPN styles. Each of the sites contains LSA lithic assemblages dominated by lithic artifacts made of locally available quartz, quartzite, and volcanic rocks. Although Kansyore sites are typically defined on the basis of ceramics, the rock shelters excavated by Gabel have been incorporated into recent discussions of Kansyore lithic variability within the Lake Victoria basin on the basis of techno-typological similarities (Seitsonen, 2010). Like other Kansyore sites (Robertshaw, 1991), obsidian artifacts are persistently present in low quantities (n=28–157, 0.26–0.98%) at the Winam Gulf rock shelters (Gabel, 1969; see SOM Table A). Our lithic artifact sample includes unretouched debitage as well as tools such as backed microliths. The fauna from the rock shelters considered here, as reported by Gabel (1969), are dominated by wild taxa (reduncine and alcelaphine bovids, bushpig,



**Fig. 8.** Discriminant functions were derived with source as the grouping variable and Zr, Rb, Nb, Sr, Mn, and Fe as predicting variables. The resulting scatterplot shows the artifacts (black squares), their six matching geological sources (colorful circles), and select other obsidian sources reported by Brown et al. (2013) without matching artifacts (various grey symbols). Like Fig. 6, the published WDXRF data from Brown et al. (2013) are the lighter shades (e.g., light green for Eburru), while our calibrated pXRF data on geological specimens (when available) are the darker shades (e.g., dark green for Eburru).



Fig. 9. Obsidian sources around Lake Naivasha that we identified at the six rock shelters in our study (cyan triangles with labels), identified by Brown et al. (2013) at other sites (red triangles), and not identified by Brown et al. (2013) at other sites (black triangles). The line between Hell's Gate 1 and Ololbutot 1 reflects that, in our view, these two obsidian sources in Brown et al. (2013) are chemically indistinguishable based on the available data (i.e., just two obsidian specimens define Hell's Gate 1). Background map: satellite image courtesy of the DigitalGlobe Foundation (© DigitalGlobe, Inc., All Rights Reserved).

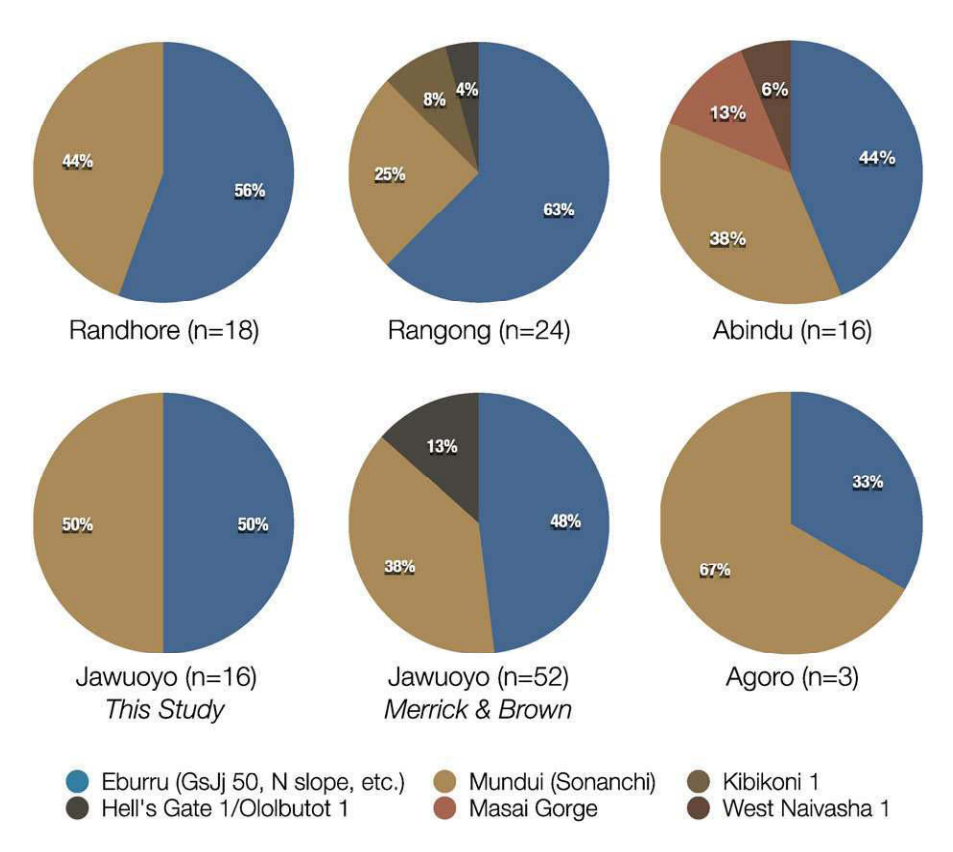


**Fig. 10.** Source identifications of obsidian artifacts (from Table 9) for five of the six rock shelters (leaving out Nyaidha, n = 1), including the Jawuoyo results from Merrick and Brown (1984b).

warthog, zebra). There are also freshwater molluscs, fish (lungfish, tilapia, catfish), and traces of domesticated animals (cattle, sheep or goat, possibly cat).

Although imperfect, evidence from the lithic, ceramic, and faunal assemblages (i.e., limited evidence for domesticates) and the available radiocarbon dates from these six rock shelters indicate the presence of late Holocene populations of foragers north of Winam Gulf. Their assemblages are at least broadly aligned with the "Late/Terminal Kansyore" of Dale and Ashley (2010), although the extent to which similarity in ceramic styles tracks other social variables at Kansyore sites remains poorly understood (Ashley and Grillo, 2015). We recognize this complexity as well as the limits of our current data, but we group our results from Randhore, Rangong, Nyaidha, Jawuoyo, Agoro, and Abindu shelters with other known "Late/Terminal Kansyore" sites to increase the total sample of chemically sourced obsidian artifacts made by late Holocene foragers in the Lake Victoria region from 88 to 166, more than doubling the number of sites from three to eight.

Obsidian artifacts in these lithic assemblages are principally bipolar pieces/debris, geometric crescents, and backed and retouched blade fragments. With almost no cores or core trimming elements and very little evidence of production debris, the assemblages are consistent with expectations for down- the-line acquisition of small blades and tools near the end of the reduction sequence, rather than the exchange

of large cores or nodules. Details regarding the types, dimensions, and identifications of the artifacts are found in SOM Table B.

#### 9. Obsidian source identifications

We made the artifacts' source assignments on three bases, which yielded the same results each time. As reported in Section 7, our calibrated pXRF values are highly correlated to the WDXRF data of Brown et al. (2013) for Zr, Rb, and Nb ( $R^2 = 0.96$ –0.99; Fig. 3a), and their relative differences are also very low (2–4% relative; Table 6). Therefore, first, we used these three elements. The simplest way to show three elements in two dimensions is using a ratio, and Fig. 6 shows a scatterplot of Zr versus Nb/Rb. Note that, for five of the six identified sources, we plot not only the WDXRF data of Brown et al. (2013) but also our calibrated pXRF measurements for geological specimens from the same sources. These specimens offered an extra check on our ability to reproduce the data in Brown et al. (2013). The published and our newly measured data tend to directly overlap in the scatterplot, demonstrating how well our measurements duplicate those from Brown et al. (2013). The data for this plot and the following ones are available in Table 8.

Second, we derived discriminant functions based on four trace elements – Zr, Rb, Nb, and Sr – to minimize within-source variance and maximize between-source variance. The artifact data were then plotted

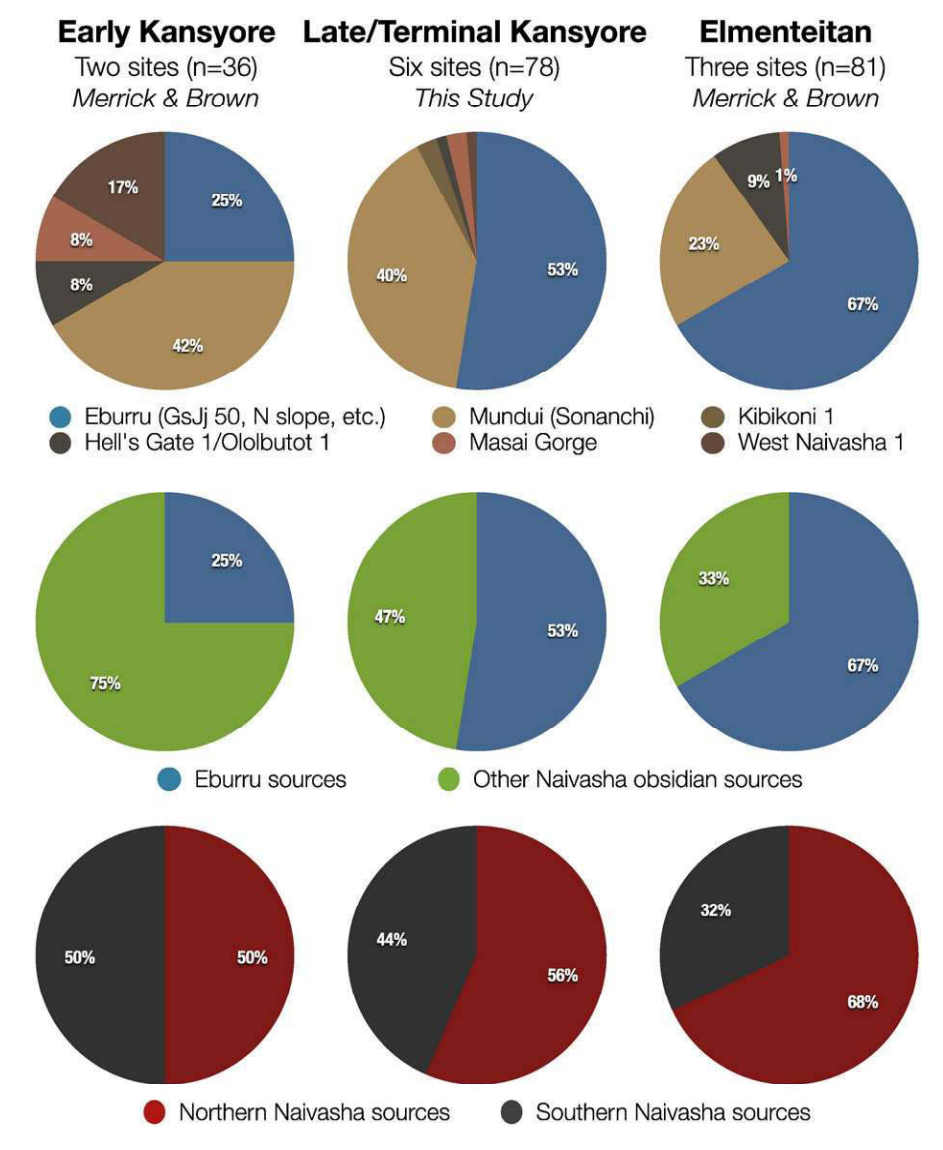


Fig. 11. Trends in obsidian source use for Early Kansyore (Merrick and Brown, 1984a, b), Late/Terminal Kansyore, and Elmenteitan (Merrick and Brown, 1984a, b) contexts.

**Table 9**Summary of our obsidian source identifications by rock shelter and the earlier Jawuoyo results from Merrick and Brown (1984b).

	This st	ıdy											
	Eburru		Mundui (Sonancl	ni)	Kibiko	ni 1	Hell's Ga 1/Ololbu		Masa	i Gorge	West N 1	laivasha	
Sites	n	%	n	%	n	%	n	%	n	%	n	%	Sum
Abindu	7	44%	6	38%					2	13%	1	6%	16
Agoro	1	33%	2	67%									3
Jawuoyo	8	50%	8	50%									16
Nyaidha			1	100%									1
Randhore	10	56%	8	44%									18
Rangong	15	63%	6	25%	2	8%	1	4%					24
Total	41	53%	31	40%	2	3%	1	1%	2	3%	1	1%	78
	Merrio	k & Brown											
Jawuoyo	25	48%	20	38%			7	13%					52

with the derived functions, and Fig. 7 shows the outcome: the same source assignments as Fig. 6, and our new measurements directly overlap with the published values from Brown et al. (2013).

Third, we derived discriminant functions based on six elements: Zr, Rb, Nb, and Sr with the addition of Fe and Mn, both of which Brown et al. (2013) measured using EMPA. Fe is one of the elements favored by Brown et al. (2013) for source identification. Our pXRF measurements are highly correlated to their EMPA data for Fe ( $R^2 = 0.99$ ; Fig. 3), and the relative differences are very low (3% on average; Table 6). Fig. 8 shows the outcome: the same source assignments as Figs. 6 and 7, and our pXRF measurements overlap with the published values from Brown et al. (2013).

Thus, our source identifications remain stable, and our measurements overlap with those of Brown et al. (2013) whether we simply use a scatterplot based on Zr, Nb, and Rb or multivariate statistical methods based on six well-measured elements.

#### 10. Interpretation

Data from Randhore, Rangong, Nyaidha, Jawuoyo, Agoro, and Abindu rock shelters exhibit approximately equal representation of obsidians from Mt. Eburru (53%) and other sources near Lake Naivasha (Figs. 9–11; Table 9). These sources are 200 km at a minimum distance from Lake Victoria and closer to  $\sim\!300-350$  km if one assumes movement around, rather than across, the Mau Escarpment. There is no evidence for a Late/Terminal Kansyore presence in the Central Rift Valley, which by  $\sim\!2$  ka was occupied by Elmenteitan and SPN pastoralists. Given apparent control of key obsidian sources by pastoralist groups within the Rift Valley and on Mt. Eburru, and the widespread dispersal of this material at pastoral sites across much of present-day Kenya and northern Tanzania, we interpret the acquisition of obsidian at late Holocene forager sites through the lens of contact and exchange. Differences in obsidian acquisition may reflect changes to regional forager interaction networks through time.

**Table 10** Comparing Z-scores and p values by period for Eburru versus other Naivasha obsidian sources. All differences are statistically significant when p=0.10; however, the Late/Terminal Kansyore versus Elmenteitan difference is not significant when p=0.05.

		Early Kansyore	Late/Terminal Kansyore	Elmenteitan
Early Kansyore	Z-score:	-	-2.757	-4.173
	p value:		0.006	0.000
Late/Terminal Kansyore	Z-score:	2.757	_	-1.813
	p value:	0.006		0.070
Early Kansyore	Z-score:	4.173	1.813	=
	p value:	0.000	0.070	

The increase in obsidian from Mt. Eburru at late Holocene sites that include Late/Terminal Kansyore ones relative to previously published data from Early Kansyore ones (Fig. 11) is strong evidence for direct interaction between Kansyore-producing forager-fishers and Elmenteitan-producing herders who migrated into the region by ~2000 cal. BP. By this time, Elmenteitan occupations had come to replace and overlay Eburran V forager levels in caves and rock shelters around Eburru (Ambrose, 1985, 1998). Much of the obsidian originating from the upper Mt. Eburru sources likely originated from the GsJj50 quarry, where recent excavations have yielded dense quarrying and workshop deposits, contemporary with the Late/Terminal Kansyore, with exclusively Elmenteitan ceramics and tools (Goldstein and Munyiri, in press). There is a lack of evidence for comparable forager activity on Mt. Eburru at this time, yet large amounts of Eburru obsidian arrived at Elmenteitan sites in the Lake Victoria basin, such as Wadh Lang'o and Gogo Falls. Social interaction with Elmenteitan pastoralist communities is the most likely explanation for how Late Kansyore and other communities of foragers acquired obsidians from these sources.

Obsidian acquisition from multiple Lake Naivasha sources occurred both prior to and during the appearance of pastoralism in the Lake Victoria region. The proportion of Mt. Eburru obsidian is lowest at Early Kansyore assemblages (25%) and highest in Elmenteitan (67%) assemblages (Fig. 11). Late/Terminal Kansyore sites (53%) are intermediate. These diachronic differences are statistically significant (Table 10). When the sources are divided into those north and south of Lake Naivasha (Figs. 9 & 11), obsidian artifacts from sources north of Lake Naivasha are least abundant at Early Kansyore assemblages (50%), most common at Elmenteitan ones (68%), with Late/Terminal Kansyore assemblages showing an intermediate value (56%). The number of sources represented in Late/Terminal Kansyore assemblages (n = 6) is greater than that in either Early Kansyore (n = 5) or Elmenteitan (n = 4) assemblages. The significance of these general trends is necessarily tempered by our small sample sizes, but the persistent use of obsidians from the Central Rift by groups in the Lake Victoria basin throughout much of the Holocene is apparent.

We have suggested that Eburru obsidian was obtained through Elmenteitan groups. How, then, did Kansyore groups acquire obsidians from the Naivasha sources? Continuity in Lake Naivasha sources through time could reflect ongoing forager networks extending from the Rift Valley, around (or over) the Mau Escarpment, and into the Nyanza region. Our understanding of the distribution and diversity in LSA foragers remains poorly understood, leaving significant potential for such networks to have persisted through the spread of food production (Wilshaw, 2016). Alternatively, SPN-producing herders were heavily exploiting Naivasha sources. The nearest known SPN sites to Lake Victoria are ~90–100 km to the southeast in the Lemek Valley (Robertshaw et al., 1990). Considering the co-occupation of Elmenteitan

and SPN groups across southwestern Kenya, it is possible there was also an as-of-yet undetected significant SPN presence closer to the Kansyore world (as appears to be the case in northern Tanzania where, at sites such as Mumba, Kansyore strata are overlain by SPN layers). Considerably more archaeological and sourcing studies are needed to test these hypotheses, which, at present, remain speculative. Nevertheless, our sourcing results support hypotheses that the Late/Terminal Kansyore fisher-foragers were engaged in a complex set of social relationships (Karega-Mũnene, 2002; Dale, 2007; Prendergast, 2008).

We suggest that the expanded access to diverse obsidians during the Late/Terminal Kansyore reflects one dimension of the broader Kansyore resilience strategy through the Holocene. If the obsidian sourcing pattern did result from interactions with a diverse range of other pastoralists and foragers, it would hint at a social flexibility that mirrors the apparent flexibility in Kansyore subsistence, settlement patterns, and ceramic production (Dale et al., 2004; Prendergast and Lane, 2010; Lane, 2004). Ethno-historically African foragers and herders have often entered into mutualistic relationships wherein the foragers are viewed as specialists in the acquisition of important subsistence supplements such as fish and honey (Berntsen, 1976; Turton, 1986; Blackburn, 2006), producers of poisons and medicines, and practitioners of magic (Kenny, 1981; Kratz, 1993; Grillo, 2014). Transfer or mimesis of material culture often accompanies these economic arrangements, with hunter-gatherers exhibiting a high degree of agency in what pastoralist materials they incorporate and the meanings of those materials in their own cultural sphere (Klumpp and Kratz, 1993). Our results provide preliminary support for a similar model existing in the past, wherein Kansyore or other fisher-foragers were able to absorb new challenges and opportunities presented by the arrival of herders while maintaining the essential structures of a foraging economy.

Pursuing evidence for forager-pastoralist interactions is of crucial importance in understanding both the trajectories of early food production in Eastern Africa and those strategies that allowed foraging to persist as a viable strategy through Holocene climatic changes (Marshall and Hildebrand, 2002; Dale et al., 2004; Gifford-Gonzalez, 1998, 2000, 2016; Marshall et al., 2011; Prendergast, 2011; Prendergast and Mutundu, 2009). In many areas, foragers and food producers alike had to survive in drought-prone, highly unpredictable environments where resources are spatially and temporally disparate. The complex social systems that likely arose among economically and socially diverse communities during the late Holocene may be better understood as mutually beneficial forms of risk mitigation and resilience (Lane, 2004; Prendergast and Mutundu, 2009; Marshall et al., 2011; Chritz et al., 2015). Our data offer supporting evidence that such relationships existed in the Lake Victoria region. This study demonstrates that obsidian sourcing has great potential to test these ideas and to develop a more comprehensive understanding of material access, exchange systems, and interaction spheres. We hope that future studies will take advantage of this opportunity to investigate such questions, which underlie key debates in studies of foragers and food production both regionally and globally.

#### 11. Concluding remarks

Regarding our calibration to and use of the WDXRF and EMPA datasets from Brown et al. (2013), elements of interest exhibit very high correlations ( $R^2=0.96$ –0.99) to our pXRF data. Once calibrated to Brown et al. (2013), our pXRF data exhibit, on average, only 2–5% relative differences, equal to or better than compatible datasets from lab-based instruments. When our pXRF data of geological specimens are plotted alongside published values from Brown et al. (2013), they directly overlap, further demonstrating compatibility. Accordingly, we can reliably and validly use pXRF in conjunction with the Brown et al. (2013) database to conduct rapid, field-based source identifications of Kenyan obsidian artifacts. Such work will be strengthened as our knowledge of Kenyan obsidian sources continues to improve via ongoing source characterization

projects (e.g., Coleman et al., 2008, 2009; Ambrose, 2012; Ambrose et al., 2012a, b; Slater et al., 2012; Slater and Ambrose, 2015).

Archaeologically this research elucidates interactions between LSA forager-fishers and pastoralists near Lake Victoria. Specifically, the extent to which obsidian acquisition in late Holocene forager contexts that includes Late/Terminal Kansyore assemblages reflects the Early Kansyore and/or Elmenteitan patterns can elucidate links between fisher-forager and pastoral populations. Thus, we present new source attributions for 78 obsidian artifacts from six contemporaneous late Holocene rock shelters along the Winam Gulf. Obsidian is scarce (0.3–1.0%) in these lithic assemblages, and our results reveal approximately equal representation of obsidian from Mt. Eburru (53%) and other sources near Lake Naivasha. Without evidence for a Kansyore presence so far east of our studied site sample, we interpret their obsidian acquisition as a reflection of intergroup contact and exchange. Interaction with Elmenteitan herders or other pastoralists is the most likely explanation for how Late/Terminal Kansyore groups acquired obsidian from the identified sources, involving culturally mediated access to this material.

The obsidian sourcing results we report here hint that the Late/Terminal Kansyore and other late Holocene fisher-foragers were engaged in a complex set of social relationships with neighboring pastoralist and farming communities. This line of evidence supports the idea that these fisher-forager communities interacted with herding groups for long periods of time but without being assimilated into food-producing lifeways. Expanded access to diverse obsidians might reflect the broader Kansyore resilience strategy in an unpredictable and drought-prone environment, and their interactions with economically and socially diverse communities hint at mutually beneficial forms of risk mitigation and resilience. Obsidian sourcing holds great potential for testing such ideas and developing a better understanding of Kansyore resource access and social spheres. The analytical tools and source databases now exist to investigate such questions, which underlie outstanding debates in studies of foragers and food production.

Supplementary data to this article can be found online at http://dx.doi.org/10.1016/j.jasrep.2017.01.001.

#### Acknowledgements

We are indebted to Frank Brown and Harry Merrick for generously contributing obsidian specimens from Brown et al. (2013), which made this study possible. Additional specimens of Kenyan obsidian, which aided our compatibility tests, were contributed by Minghua Ren and were collected by Elizabeth Anthony and Jesus Velador, University of Texas-El Paso. We thank Curtis Runnels, Director, and Priscilla Murray, Curator, for access to the artifacts in the Gabel Museum of Archaeology at Boston University. Funding support was provided by the American School for Prehistoric Research and by Harvard University. Frahm's work was supported, in part, by the Department of Anthropology, Department of Earth Sciences, Institute for Rock Magnetism, Electron Microprobe Laboratory at the University of Minnesota. Research assistance was provided by Ravid Ekshtain and Liev Frahm. The pXRF instrument used in this study is part of the research infrastructure of the University of Minnesota's Wilford Laboratory of North American Archaeology, directed by Katherine Hayes. Funding for the instrument was provided by the College of Liberal Arts and by the Office of the Associate Dean for Research and Graduate Programs. We thank Nick Blegen, Matt Magnani, and especially Mary Prendergast for their constructive critiques of earlier drafts of this paper. Two anonymous reviewers provided helpful comments that improved the final version.

#### References

Adler, D.S., Wilkinson, K., Blockley, S., Mark, D., Pinhasi, R., Schmidt-Magee, B., Nahapetyan, S., Mallol, C., Berna, F., Glauberman, P., Raczynski-Henk, Y., Cullen, V., Frahm, E., Jöris, O., Macloud, A., Smith, V., Gasparyan, B., 2014. Early Levallois technology and the transition from the Lower to Middle Palaeolithic in the southern Caucasus. Science 345 (6204), 1609–1613.

- Ambrose, S.H., 1984. The introduction of pastoral adaptations to the highlands of East Africa. In: Clark, J.D., Brandt, S.A. (Eds.), From Hunters to Farmers: The Causes and Consequences of Food Production in Africa. University of California Press, Berkeley, pp. 212–239.
- Ambrose, S.H., 1985. Excavations at Masai Gorge rockshelter, Naivasha. Azania 20, 29–67.
  Ambrose, S.H., 2001. Middle and Later Stone Age settlement patterns in the Central Rift Valley, Kenya: comparisons and contrasts. In: Conard, N.J. (Ed.), Settlement Dynamics of the Middle Paleolithic and MiddleStoneAge. Tubingen, Kerns Verlag, pp. 21–24.
- Ambrose, S.H., 1998. Chronology of the Later Stone Age and food production in East Africa. I. Archaeol. Sci. 25. 377–392.
- Ambrose, S.H., 2012. Obsidian hydration dating and source exploitation studies in Africa. In: Liritzis, I., Stevenson, C.M. (Eds.), The Dating and Provenance of Obsidian and Ancient Manufactured Glasses. University of New Mexico Press, Alberquerque, pp. 56–72.
- Ambrose, S.H., Ferguson, J., Glascock, M., Slater, P., 2012a. Chemical Fingerprinting of Kenyan Obsidian Sources and Late Quaternary Artifacts with NAA and XRF Presented at the Annual Meeting of the Society for American Archaeology, Memphis, Tennessee.
- Ambrose, S.H., Slater, P., Ferguson, J., Glascock, M., Steele, I., 2012b. Obsidian Source Survey and Late Quaternary Artifact Sourcing in Kenya: Implications for Early Modern Human Behaviour Presented at the Annual Meeting of the Palaeoanthropology Society, Memphis, Tennessee.
- Ashley, C.Z., Grillo, K.M., 2015. Archaeological ceramics from eastern Africa: past approaches and future directions. Azania 50, 460–480.
- Berntsen, J.L., 1976. The Maasai and their neighbors: variables of interaction. Afr. Econ. Hist. 2, 1–11.
- Blackburn, R.H., 2006. Fission, fusion, and foragers in East Africa: micro- and macroprocesses of diversity and integration among Okiek groups. Cultural Diversity Among Twentieth-century Foragers: An African Perspective, pp. 188–212.
- Bower, J.R.F., Nelson, C.M., Waibel, A.F., Wandibba, S., 1977. The University of Massachusetts' Later Stone Age/Pastoral 'Neolithic' comparative study in central Kenya: an overview. Azania 12, 119–146.
- Brandt, S.A., 2015. Not Always Shiny and Pretty: The Darker Side of Obsidian in Symbolizing Power, Ethnicity, and Inequality in Contemporary Ethiopia Presented at the Annual Meeting of the Society for American Archaeology, San Francisco, California.
- Brandt, S.A., Johnson, L.M., 2011. Lithics, Community Organization, and Early State Formation at the Pre-Aksumite Site of Mezber, NE Ethiopia Presented at the Annual Meeting of the Society for American Archaeology, Sacramento, California.
- Brandt, S.A., Weedman, K.J., 1997. The ethnoarchaeology of hideworking and flake stone-tool use in southern Ethiopia. Ethiopia in Broader Perspective: Papers of the XIIIth International Conference of Ethiopian Studies, Kyoto, 12–17 December 1997, pp. 351–361.
- Brandt, S.A., Weedman, K.J., Hundie, G., 1996. Gurage hideworking, stone-tool use, and social identity: an ethnoarchaeological perspective. Essays on Gurage Language and Culture: Dedicated to Wolf Leslau on the Occasion of His 90th Birthday, November 14th, 1996, pp. 35–51.
- Brandt, S.A., Johnson, L.M., Chase, A., 2013. A comparative study of multiple Bruker Tracer III calibrated instruments using identical analytical and operational procedures: implications for past, present, and future obsidian studies. 78th Annual Meeting, Honolulu, Hawaii, 3–7 April 2013. Society for American Archaeology.
- Brandt, S.A., Ferguson, J., Johnson, L.M., 2014. Lithic Raw Material Acquisition, Ethnicity and Source/Settlement Location: An Ethnoarchaeological Study of Ethiopian Craftspeople Presented at the Annual Meeting of the Society for American Archaeology, Austin, Texas.
- Brown, F.H., Haileab, B., McDougall, I., 2006. Sequence of tuffs between the KBS Tuff and the Chari Tuff in the Turkana Basin, Kenya and Ethiopia. J. Geol. Soc. Lond. 163, 185–204.
- Brown, F.H., Nash, B.P., Fernandez, D.P., Merrick, H.V., Thomas, R.J., 2013. Geochemical composition of source obsidians from Kenya. J. Archaeol. Sci. 40, 3233–3251.
- Burley, D.V., Sheppard, P.J., Simonin, M., 2011. Tongan and Samoan volcanic glass: pXRF analysis and implications for constructs of ancestral Polynesian society. J. Archaeol. Sci. 38 (10), 2625–2632.
- Cann, J.R., Renfrew, C., 1964. The characterization of obsidian and its application to the Mediterranean region. Proc. Prehist. Soc. 30, 111–133.
- Carter, T., 2009. Elemental characterization of Neolithic artefacts using portable X-ray fluorescence. Çatalhöyük Research Project: Çatalhöyük 2009 Archive Report, pp. 126–128.
- Carter, T., Contreras, D., 2012. The character and use of the Soros Hill obsidian source, Antiparos (Greece). C.R. Palevol 11, 595–602.
- Carter, T., Shackley, M.S., 2007. Sourcing obsidian from Neolithic Catalhoyuk (Turkey) using energy dispersive X-ray fluorescence. Archaeometry 49 (3), 437–454.
- Carter, T., Grant, S., Kartal, M., Özkaya, V., Coşkun, A., 2013. Networks and Neolithisation: sourcing obsidian from Körtik Tepe (SE Anatolia). J. Archaeol. Sci. 40 (1), 556–569.
- Cecil, L.G., Moriarity, M.D., Speakman, R.J., Glascock, M.D., 2007. Feasibility of field-portable XRF to identify obsidian sources in central Peten, Guatemala. In: Glascock, M.D., Speakman, R.J., Popelka-Filcoff, R.S. (Eds.), Archaeological Chemistry: Analytical Techniques and Archaeological InterpretationACS Symposium Series No. 968. American Chemical Society, Washington, DC, pp. 506–521.
- Cesareo, R., Ridolfi, S., Marabelli, M., Castellano, A., Buccolieri, G., Donativi, M., Gigante, G.E., Brunetti, A., Medina, M.A.R., 2008. Portable systems for energy-dispersive X-ray fluorescence analysis of works of art. In: Potts, P.J., West, M. (Eds.), Portable X-ray Fluorescence Spectrometry: Capabilities for In Situ Analysis. The Royal Society of Chemistry, Cambridge, pp. 206–246.
- Chritz, K.L., Marshall, F., Zagal, M., Kirera, F., Cerling, T.E., 2015. Environments and try-panosomiasis risks for early herders in the later Holocene of the Victoria Basin, Kenya. Proc. Natl. Acad. Sci. 112 (12), 3674–3679.

- Clark, J.D., Kurashina, H., 1981. A study of the work of a modern tanner in Ethiopia and its relevance for archaeological interpretation. In: Gould, R.A., Schiffer, M.B. (Eds.), Modern Material Culture: The Archaeology of Us. Academic Press, pp. 303–343.
- Coleman, M.E., Ferguson, J.R., Glascock, M.D., Robertson, J.D., Ambrose, S.H., 2008. A new look at the geochemistry of obsidian from East Africa. Int. Assoc. Obsidian Stud. Bull. 39, 11–14.
- Coleman, M., Robertson, J.D., Ferguson, J., Glascock, M.D., Ambrose, S.H., 2009. Further Studies Into the Geochemistry of Obsidian From Kenya Presented at the Annual Meeting of the Society for American Archaeology, Atlanta, Georgia.
- Craig, N., Speakman, R.J., Popelka-Filcoff, R., Glascock, M.D., Robertson, J., Shackley, M.S., Aldenderfer, M., 2007. Comparison of XRF and PXRF for analysis of archaeological obsidian from southern Perú. J. Archaeol. Sci. 34, 2012–2024.
- Craig, N., Speakman, R.J., Popelka-Filcoff, R., Aldenderfer, M., Blanco, L., Vega, M., Glascock, M.D., Stanish, C., 2010. Macusani obsidian from southern Peru: a characterization of its elemental composition with a demonstration of its ancient use. J. Archaeol. Sci. 37, 569–576.
- Dale, D., 2007. An Archaeological Investigation of the Kansyore, Later Stone Age Hunter-Gatherers in East Africa. (Ph.D. thesis). Washington University, St. Louis, MO.
- Dale, D., Ashley, C.Z., 2010. Holocene hunter-fisher-gatherer communities: new perspectives on Kansyore using communities of western Kenya. Azania 45 (1), 24–48.
- Dale, D., Marshall, F., Pilgram, T., 2004. Delayed-return hunter-gatherers in Africa? Historic perspectives from the Okiek and archaeological perspectives from the Kansyore. Hunters and Gatherers in Theory and Archaeology, pp. 340–375.
- de Boer, D.K.G., Brouwer, P.N., 1990. Adv. X-ray Anal. 33, 237-243.
- Dillian, C.D., Bello, C.A., Shackley, M.S., 2010. Long-distance exchange of obsidian in the Mid-Atlantic United States. In: Dillian, C., White, C. (Eds.), Trade and Exchange: Archaeological Studies From Prehistory and History. Springer, New York, pp. 17–35.
- Doronicheva, E.V., Shackley, M.S., 2014. Obsidian exploitation strategies in the Middle and Upper Paleolithic of the northern Caucasus: new data from Mesmaiskaya Cave. Paleo-Anthropology 2014, 565–585.
- Ebert, C.E., Dennison, M., Hirth, K.G., McClure, S.B., Kennett, D.J., 2014. Formative period obsidian exchange along the Pacific coast of Mesoamerica. Archaeometry 57 (Suppl. 1), 54–73.
- Eggins, S.M., 2003. Laser ablation ICP-MS analysis of geological materials prepared as lithium borate glasses. Geostand. Newslett. 27, 147–162.
- Faith, J.T., Tryon, C.A., Peppe, D.J., Beverly, E.J., Blegen, N., Blumenthal, S., Chritz, K.L., Driese, S.G., Patterson, D., 2015. The Middle Stone Age archaeological and paleoenvironmental record from Karungu, Lake Victoria basin, Kenya. J. Hum. Evol. 83, 28–45.
- Ferguson, J.R., 2012. Chapter 12: X-ray fluorescence of obsidian: approaches to calibration and the analysis of small samples. In: Shugar, A.N., Mass, J.L. (Eds.), Handheld XRF for Art and Archaeology. Leuven University Press, Leuven, pp. 401–422.
- Forster, N., Grave, P., 2012. Non-destructive PXRF analysis of museum-curated obsidian from the Near East. J. Archaeol. Sci. 39, 728–736.
- Frahm, E., 2007. An evaluation of portable X-ray fluorescence for artifact sourcing in the field: can a handheld device differentiate Anatolian obsidian sources? Session: sourcing techniques in archaeology. Geological Society of America Abstracts With Programs. 39, p. 29 (Denver, Colorado).
- Frahm, E., 2013. Validity of "off-the-shelf" handheld portable XRF for sourcing Near Eastern obsidian chip debris. J. Archaeol. Sci. 40, 1080–1092.
- Frahm, E., 2014a. Characterizing obsidian sources with portable XRF: accuracy, reproducibility, and field relationships in a case study from Armenia. J. Archaeol. Sci. 49, 105–125.
- Frahm, E., 2014b. Chapter 8: what constitutes an obsidian "source"?: landscape and geochemical considerations and their archaeological implications. In: Dillian, C. (Ed.), Twenty-Five Years on the Cutting Edge of Obsidian Studies. International Association for Obsidian Studies, pp. 49–70.
- Frahm, E., Feinberg, J.M., 2013a. From flow to quarry: magnetic properties of obsidian and changing the scales of archaeological sourcing. J. Archaeol. Sci. 40, 3706–3721.
- Frahm, E., Feinberg, J.M., 2013b. Empires and resources: central Anatolian obsidian at Urkesh (Tell Mozan, Syria) during the Akkadian period. J. Archaeol. Sci. 40 (2), 1122–1135.
- Frahm, E., Feinberg, J.M., 2013c. Environment and collapse: eastern Anatolian obsidians at Urkesh (Tell Mozan, Syria) and the third-millennium Mesopotamian urban crisis. J. Archaeol. Sci. 40 (4), 1866–1878.
- Frahm, E., Feinberg, J.M., 2015. Reassessing obsidian field relationships at Glass Buttes, Oregon. J. Archaeol. Sci. Rep. 2, 654–665.
- Frahm, E., Doonan, R.C.P., Kilikoglou, V., 2014a. Handheld portable X-ray fluorescence of Aegean obsidians. Archaeometry 56, 228–260.
- Frahm, E., Feinberg, J.M., Schmidt-Magee, B., Wilkinson, K., Gasparyan, B., Yeritsyan, B., Karapetian, S., Meliksetian, K., Muth, M.J., Adler, D.S., 2014b. Sourcing geochemically identical obsidian: multiscalar magnetic variations in the Gutansar volcanic complex and implications for Palaeolithic research in Armenia. J. Archaeol. Sci. 47, 164–178.
- Frahm, E., Schmidt, B., Gasparyan, B., Yeritsyan, B., Karapetian, S., Meliksetian, K., Adler, D.S., 2014c. Ten seconds in the field: rapid Armenian obsidian sourcing with portable XRF to inform excavations and surveys. J. Archaeol. Sci. 41, 333–348.
- Gabel, C., 1969. Six rock shelters on the northern Kavirondo shore of Lake Victoria. Afr. Hist. Stud. 2 (2), 205–254.
- Galipaud, J.-C., Reepmeyer, C., Torrence, R., Kelloway, S., White, P., 2014. Long-distance connections in Vanuatu: new obsidian characterisations for the Makué site, Aore Island. Archaeol. Ocean. 49, 110–116.
- Gifford-Gonzalez, D., 1998. Early pastoralists in East Africa: ecological and social dimensions. J. Anthropol. Archaeol. 17 (2), 166–200.
- Gifford-Gonzalez, D., 2000. Animal disease challenges to the emergence of pastoralism in sub-Saharan Africa. Afr. Archaeol. Rev. 17 (3), 95–139.
- Gifford-Gonzalez, 2016. "Animal disease challenges" fifteen years later: the hypothesis in light of new data. Quat. Int. http://dx.doi.org/10.1016/j.quaint.2015.10.054 (In Press).

- Glascock, M.D., 1994. New World obsidian: recent investigations. In: Scott, D.A., Meyers, P. (Eds.), Archaeometry of Pre-Columbian Sites and Artifacts. Getty Trust, pp. 113–134.
- Glascock, M.D., 1999. An inter-laboratory comparison of element compositions for two obsidian sources. Int. Assoc. Obsidian Stud. Bull. 23, 13-25.
- Glascock, M.D., 2011. Chapter 8: comparison and contrast between XRF and NAA: used for characterization of obsidian sources in central Mexico. In: Shackley, M.S. (Ed.), X-ray Fluorescence Spectrometry (XRF) in Geoarchaeology. Springer, pp. 161–192.
- Glascock, M.D., Ferguson, J.R., 2012. Report on the Analysis of Obsidian Source Samples by Multiple Analytical Methods. MURR Archaeometry Laboratory Report.
- Goldstein, S.T., Munyiri, J.M. In press. The Upper Opuru Quarry Site (GsJj50): New perspectives on obsidian access and exchange during the Pastoral Neolithic of southern Kenya, African Archaeological Review.
- Goldstein, S.T., 2014. Quantifying endscraper reduction in the context of obsidian exchange among early pastoralists in southwestern Kenya. Lithic Technol. 39 (1), 3-19.
- Golitko, M., 2011. Provenience investigations of ceramic and obsidian samples using laser ablation inductively coupled plasma mass spectrometry and portable X-ray fluorescence, Fieldiana Anthropol, 42, 251-287.
- Golitko, M., Meierhoff, J., Terrell, J.E., 2010. Chemical characterization of sources of obsidian from the Sepik coast (PNG). Archaeol. Ocean. 45 (3), 120-129.
- Golitko, M., Schauer, M., Terrell, J.E., 2012. Identification of Fergusson Island obsidian on
- the Sepik coast of northern Papua New Guinea. Archaeol. Ocean. 47, 151–156. Goodale, N., Bailey, D., Jones, G., Prescott, C., Scholz, E., Stagliano, N., Lewis, C., 2012. pXRF: a study of inter-instrument performance. J. Archaeol. Sci. 39, 875–883.
- Green, R.C., 1998. A 1990s perspective on method and theory in archaeological volcanic glass studies. In: Shackley, M.S. (Ed.), Archaeological Obsidian Studies: Method and Theory. Plenum Press, New York, pp. 223-235.
- Grillo, K.M., 2014. Pastoralism and pottery use: an ethnoarchaeological study in Samburu, Kenya. Afr. Archaeol. Rev. 31 (2), 105-130.
- Harbottle, G., 1982. Chemical characterization in archaeology. In: Ericson, J., Earle, T.K. (Eds.), Contexts for Prehistoric Exchange. Academic Press, New York, pp. 13-51.
- Heginbotham, A., Bezur, A., Bouchard, M., Davis, J.M., Eremin, K., Frantz, J.H., Glinsman, L., Hayek, L.-A., Hook, D., Kantarelou, V., Germanos Karydas, A., Lee, L., Mass, J., Matsen, C., McCarthy, B., McGath, M., Shugar, A., Sirois, J., Smith, D., Speakman, R.J., 2010. In: Mardikian, P., et al. (Eds.), An evaluation of inter-laboratory reproducibility for quantitative XRF of historic copper alloys. Proceedings of the International Conference on Metal Conservation, Charleston, South Carolina, USA, October 11-15, 2010. Clemson University Press, pp. 244-255.
- Horwitz, W., Kamps, L.R., Boyer, K.W., 1980. Quality assurance in the analysis of foods and trace constituents. J. Assoc. Off. Anal. Chem. 63, 1344-1354.
- Hughes, R.E., 1998. On reliability, validity, and scale in obsidian sourcing research. In: Ramenofsky, A.F., Steffen, A. (Eds.), Unit Issues in Archaeology: Measuring Time, Space, and Material. University of Utah Press, pp. 103-114.
- Hughes, R., 2007. The geologic sources of obsidian artifacts from Minnesota archaeological sites. The Minnesota Archaeologist 66, 53-68.
- Hughes, R.E., Smith, R.L., 1993. Archaeology, geology, and geochemistry of obsidian provenance studies. In: Stein, J.K., Linse, A.R. (Eds.), Effects of Scale on Archaeological and Geological Perspectives, GSA Special Paper 283. Geological Society of America, Boulder, Colorado, pp. 79-91.
- Jia, P., Doelman, T., Chen, C., Zhao, H., Lin, S., Torrence, R., Glascock, M.D., 2010. Moving sources: a preliminary study of volcanic glass artifact distributions in northeast China using PXRF. J. Archaeol. Sci. 37, 1670-1677.
- Jia, P.W., Doelman, T., Torrence, R., Glascock, M.D., 2013. New pieces: the acquisition and distribution of volcanic glass sources in northeast China during the Holocene. J. Archaeol. Sci. 40, 971–982.
- Jochum, K.P., et al., 2006. MPI-DING reference glasses for in-situ microanalysis: new reference values for element concentrations and isotope ratios. Geochem. Geophys.
- Karega-Munene, 2002. Holocene foragers, fishers, and herders of western Kenya. Cambridge Monographs in African History. BAR International Series 1037 54
- Kellett, L.C., Golitko, M., Bauer, B.S., 2013. A provenance study of archaeological obsidian from the Andahuaylas region of southern Peru. J. Archaeol. Sci. 40, 1890-1902.
- Kenny, M.G., 1981. Mirror in the forest: the Dorobo hunter-gatherers as an image of the other. Africa 51 (01), 477-495.
- Klumpp, D., Kratz, C., 1993. Aesthetics, expertise and ethnicity: Okiek and Maasai perspectives on personal ornament. Being Maasai: Ethnicity and Identity in East Africa. East African Educational Publishers, Nairobi, pp. 195-221.
- Kratz, C.A., 1993. "We've always done it like this... except for a few details": "tradition" and "innovation" in Okiek ceremonies. Comp. Stud. Soc. Hist. 35 (01), 30-65.
- Kuehne, S.C., Froese, D.G., Shane, P.A.R., 2011. The INTAV intercomparison of electronbeam microanalysis of glass by tephrochronology laboratories: results and recommendations. Quat. Int. 246, 19-47.
- Kuper, R., Kröpelin, S., 2006. Climate-controlled Holocene occupation in the Sahara: motor of Africa's evolution. Science 313 (5788), 803-807.
- Kusimba, S.B., 2013. Hunter-gatherer fishers of eastern and south-central Africa since 20,000 years ago. The Oxford Handbook of African Archaeology, p. 461.
- Laidley, R.A., McKay, D., 1971. Geochemical examination of obsidians from Newberry Caldera, Oregon. Contrib. Mineral. Petrol. 30 (4), 336-342.
- Lane, P., 2004. The 'moving frontier' and the transition to food production in Kenya. Azania 39, 243-264.
- Lane, P., Ashley, C., Seitsonen, O., Harvey, P., Mire, S., Odede, F., 2007. The transition to farming in eastern Africa: new faunal and dating evidence from Wadh Lang'o and Usenge, Kenya, Antiquity 81, 62-81.
- Lawrence, M., McCoy, M.D., Barber, I., Walter, R., 2014. Geochemical sourcing of obsidians from the Pūrākaunui site, South Island, New Zealand. Archaeol. Ocean. 49, 158-163,

- Le Maitre, R.W., Streckeisen, A., Zanettin, B., Le Bas, M.J., Bonin, B., Bateman, P., Bellieni, G., Dudek, A., Schmid, R., Sorensen, H., Woolley, A.R., 2002. Igneous rocks. A Classification and Glossary of Terms: Recommendations of the International Union of Geological Sciences Subcommission of the Systematics of Igneous Rocks, second ed. Cambridge University Press, Cambridge, pp. 225-236.
- Leakey, M.D., 1945. Report on the excavations at Hyrax Hill, Nakuru, Kenya Colony, 1937– 1938. Trans. R. Soc. S. Afr. 30, 271-409.
- Leakey, M.D., 1971. Olduvai Gorge. Excavations in Beds I and II, 1960–1963 3. Cambridge University Press, Cambridge.
- Liritzis, I., 2008. Assessment of Aegean obsidian sources by a portable ED-XRF analyser: grouping, provenance and accuracy. In: Facorellis, Y., Zacharias, N., Polikreti, K. (Eds.), Proceedings of the 4th Symposium of the Hellenic Society for ArchaeometryBAR International Series 1746 (Oxford).
- Liritzis, I., Zacharias, N., 2011. Chapter 6: portable XRF of archaeological artifacts: current research, potentials and limitations. In: Shackley, M.S. (Ed.), X-ray Fluorescence Spectrometry (XRF) in Geoarchaeology. Springer, pp. 109-142.
- Lucas, A., 1942. Obsidian. Annales du Service des Antiquités de l'Egypte 41, 271–275.
- Lucas, A., 1947. Obsidian. Annales du Service des Antiquités de l'Egypte 47, 113-123.
- Marshall, F., Hildebrand, E., 2002. Cattle before crops: the beginnings of food production in Africa. J. World Prehist. 16 (2), 99-143.
- Marshall, F., Stewart, K., 1994. Hunting, fishing, and herding pastoralists of western Kenya: the fauna from Gogo Falls. Archaeozoologia 7 (1), 7-27.
- Marshall, F., Grillo, K., Arco, L., 2011. Prehistoric pastoralists and social responses to climatic risk in East Africa. Sustainable Lifeways: Cultural Persistence in an Ever-changing Environment, pp. 39-74.
- McCoy, M.D., Mills, P., Lundblad, S., Rieth, T., Kahn, J., Gard, R., 2011. A cost surface model of volcanic glass quarrying and exchange in Hawai'i. J. Archaeol. Sci. 38, 2547-2560
- McCoy, M.D., Ladefoged, T.N., Codlin, M., Sutton, D.G., 2014. Does Carneiro's circumscription theory help us understand Maori history? An analysis of the obsidian assemblage from Pouerua Pa, New Zealand (Aotearoa). J. Archaeol. Sci. 42, 467-475.
- Merrick, H.V., Brown, F.H., 1984a. Rapid chemical characterization of obsidian artifacts by electron microprobe analysis. Archaeometry 26 (2), 230-236.
- Merrick, H.V., Brown, F.H., 1984b. Obsidian sources and patterns of source utilization in Kenya and northern Tanzania: some initial findings. Afr. Archaeol. Rev. 2, 129-152
- Merrick, H.V., Brown, F.H., Connelly, M., 1988. Sources of the obsidian at Ngamuriak and other southwestern Kenyan sites. In: Robertshaw, P. (Ed.), Early Pastoralists of South-western Kenya. British Institute of Eastern Africa, Nairobi.
- Merrick, H.V., Brown, F.H., Nash, W.P., 1994. Use and movement of obsidian in the Early and Middle Stone Ages of Kenya and northern Tanzania. In: Childs, S.T. (Ed.), Society, Culture, and Technology in Africa. Masca Research Papers in Science and Archaeology, pp. 29-44.
- Milić, M., 2014. PXRF characterisation of obsidian from central Anatolia, the Aegean and central Europe. J. Archaeol. Sci. 41, 285-296
- Millhauser, J., Rodríguez-Alegría, E., Glascock, M.D., 2011. Testing the accuracy of portable X-ray fluorescence to study Aztec and colonial obsidian supply at Xaltocan, Mexico. J. Archaeol. Sci. 38, 3141-3152.
- Millhauser, J.K., Fargher, L.F., Heredia Espinoza, V.Y., Blanton, R.E., 2015. The geopolitics of obsidian supply in postclassic Tlaxcallan: a portable X-ray fluorescence study. J. Archaeol. Sci. 58, 133-146.
- Mills, B.J., Clark, J.J., Peeples, M.A., Haas, W.R., Roberts, J.M., Hill, J.B., Huntley, D.L., Borck, L., Breiger, R.L., Clauset, A., Shackley, M.S., 2013. Transformation of social networks in the late pre-Hispanic US southwest. PNAS 110 (15), 5785-5790.
- Moholy-Nagy, H., Meierhoff, J., Golitko, M., Kestle, C., 2013. An analysis of pXRF obsidian attributions from Tikal, Guatemala. Lat. Am. Antiq. 24 (1), 72-97.
- Mulrooney, M.A., McAlister, A., Stevenson, C.M., Morrison, A.E., Gendreau, L., 2014. Sourcing Rapa Nui mata'a from the collections of Bishop Museum using non-destructive pXRF. J. Polyn. Soc. 123 (3), 301-338.
- Nash, W.P., 1992. Analysis of oxygen with the electron microprobe: applications to hydrated glass and minerals. Am. Mineral. 77, 453-457.
- Nash, B.P., Merrick, H.V., Brown, F.H., 2011. Obsidian types from Holocene sites around Lake Turkana, and other localities in northern Kenya. J. Archaeol. Sci. 38 (6), 1371-1376
- Ndiema, K.E., Dillian, C.D., Braun, D.R., Harris, J.W.K., Kiura, P.W., 2011. Transport and subsistence patterns at the transition to pastoralism, Koobi Fora, Kenya. Archaeometry
- Neff, H., 1998. Units in chemistry-based ceramic provenance investigations. In: Ramenofsky, A.F., Steffen, A. (Eds.), Unit Issues in Archaeology: Measuring Time, Space, and Material. University of Utah Press, pp. 115-127.
- Negash, A., Shackley, M.S., 2006. Geochemical provenance of obsidian artefacts from the MSA site of Porc Epic, Ethiopia. Archaeometry 48 (1), 1-12.
- Ogburn, D.E., Connell, S., Gifford, C., 2009. Provisioning of the Inka army in wartime: obsidian procurement in Pambamarca, Ecuador. J. Archaeol. Sci. 36, 740-751.
- Pessanha, S., Guilherme, A., Carvalho, M.L., 2009. Comparison of matrix effects on portable and stationary XRF spectrometers for cultural heritage samples. Appl. Phys. A 97,
- Piperno, M., Collina, C., Gallotti, R., Raynal, J.-P., Kieffer, G., Le Bourdonnec, F.-X., Poupeau, G., Geraads, D., 2009. Obsidian exploitation and utilization during the Oldowan at Melka Kunture (Ethiopia). In: Hovers, E., Braun, D.R. (Eds.), Interdisciplinary Approaches to the Oldowan. Springer, Netherlands, pp. 111-128.
- Potts, P.J., West, M., 2008. Portable X-ray Fluorescence Spectrometry: Capabilities for In Situ Analysis. RSC Publishing, London.
- Prendergast, M.E., 2008. Forager Variability and Transitions to Food Production in Secondary Settings: Kansyore and Pastoral Neolithic Economies in East Africa. (Ph.D. thesis). Harvard University, Cambridge, MA.

- Prendergast, M.E., 2010. Kansyore fisher-foragers and transitions to food production in East Africa: the view from Wadh Lang'o, Nyanza Province, western Kenya. Azania 45 (1), 83–111.
- Prendergast, M.E., 2011. Hunters and herders at the periphery: the spread of herding in eastern Africa. People and Animals in Holocene Africa: Recent Advances in Archaeozoology. 2, p. 43.
- Prendergast, M.E., Lane, P.J., 2010. Middle Holocene fishing strategies in East Africa: zooarchaeological analysis of Pundo, a Kansyore shell midden in northern Nyanza (Kenya). Int. J. Osteoarchaeol. 20 (1), 88–112.
- Prendergast, M.E., Mutundu, K.K., 2009. Late Holocene zooarchaeology in East Africa: ethnographic analogues and interpretive challenges. Documenta Archaeobiologiae 7,
- Prendergast, M.E., Grillo, K.M., Mabulla, A.Z.P., Wang, H., 2014. New dates for Kansyore and Pastoral Neolithic ceramics in the Eyasi Basin. J. Afr. Archaeol. 12 (1), 89–98.
- Reimer, R., 2015. Reassessing the role of Mount Edziza obsidian in northwestern North America. J. Archaeol. Sci. Rep. 2, 418–426.
- Ren, M., Omenda, P.A., Anthony, E.Y., White, J.C., Macdonald, R., Bailey, D.K., 2006. Application of the QUILF thermobarometer to the peralkaline trachytes and pantellerites of the Eburru volcanic complex, East African Rift, Kenya. Lithos 91, 109–124.
- Robertshaw, P.T., 1988. The Elmenteitan: an early food-producing culture in East Africa. World Archaeol. 20 (1), 57–69.
- Robertshaw, P.T., 1991. Gogo Falls: excavations at a complex archaeological site east of Lake Victoria. Azania 26, 63–195.
- Robertshaw, P.T., Collett, D., Gifford, D., Mbae, B.N., 1983. Shell middens on the shores of Lake Victoria. Azania 18, 1–43.
- Robertshaw, P.T., Pilgram, T., Siiriäinen, A., Marshall, F.B., 1990. Archaeological surveys and prehistoric settlement systems. In: Robertshaw, P. (Ed.), Early Pastoralists of South-western Kenya. British Institute in Eastern Africa, Nairobi, pp. 261–266.
- Rodríguez-Alegría, E., Millhauser, J.K., Stoner, W.D., 2013. Trade, tribute, and neutron activation: the colonial political economy of Xaltocan, Mexico. J. Anthropol. Archaeol. 32 (4), 397–414.
- Scharlotta, I., 2010. Groundmass microsampling using laser ablation time-of-flight inductively coupled plasma mass spectrometry (LA-TOF-ICP-MS): potential for rhyolite provenance research. J. Archaeol. Sci. 37, 1929–1941.
- Seitsonen, O., 2010. Lithics use at Kansyore sites in East Africa: technological organization at four recently excavated sites in Nyanza Province, Kenya. Azania 45 (1), 49–82.
- Shackley, M.S., 1995. Sources of archaeological obsidian in the Greater American Southwest: an update and quantitative analysis. Am. Antiq. 60 (3), 531–551.
- Shackley, M.S., 2005. Obsidian: Geology and Archaeology in the North American Southwest. University of Arizona.
- Shackley, M.S., 2009. Intersource and intrasource geochemical variability in two newly discovered archaeological obsidian sources in the southern Great Basin. J. Calif. Gt. Basin Anthropol. 16 (1), 118–129.
- Shackley, M.S., 2011a. Chapter 2: an introduction to X-ray fluorescence (XRF) analysis in archaeology. In: Shackley, M.S. (Ed.), X-ray Fluorescence Spectrometry (XRF) in Geoarchaeology. Springer, pp. 7–44.
- Shackley, M.S., 2011b. Sources of archaeological dacite in northern New Mexico. J. Archaeol. Sci. 38, 1001–1007.
- Shackley, M.S., 2012a. An X-ray Fluorescence Analysis of Major, Minor, and Trace Element Composition of Andesite and Dacite Source Rocks From Northern New Mexico. Report Prepared for Dr. Robert Dello-Russo. Office of Archaeological Studies, Museum of New Mexico, Santa Fe.
- Shackley, M.S., 2012b. Portable X-ray fluorescence spectrometry (pXRF): the good, the bad, and the ugly (online essay). Archaeology Southwest Magazine. 26 (Spring issue).

- Sheppard, P., Trichereau, B., Milicich, C., 2010. Pacific obsidian sourcing by portable XRF. Archaeol. Ocean. 45, 21–30.
- Sheppard, P., Irwin, G., Lin, S., McCaffrey, C., 2011. Characterization of New Zealand obsidian using PXRF. J. Archaeol. Sci. 38, 45–56.
- Sherman, J., 1955. The theoretical derivation of fluorescent X-ray intensities from mixtures. Spectrochim. Acta 7, 283–306.
- Siiriäinen, A., 1990. Excavations of Elmenteitan sites in the Oldorotua Valley. In: Robertshaw, P.T. (Ed.), Early Pastoralists of South-western Kenya. Memoirs of the British Institute in Eastern Africa Memoir 11, pp. 261–279 (Nairobi).
- Skinner, C.E., Davis, M.K., 1996. X-ray Fluorescence Analysis of an Obsidian Biface From the Fort Hill Site, Highland County, Ohio Report 1996-48 prepared for the Ohio Historical Society, Columbus, Ohio, by Northwest Research Obsidian Studies Laboratory, Corvallis. Oregon.
- Slater, P., Ambrose, S.H., 2015. Technological Organization Strategies During the East African Late Stone Age: Blade Production and the Evolution of Standardized Technology Presented at the Annual Meeting of the Society for American Archaeology, San Francisco. California.
- Slater, P., Ambrose, S.H., Steele, I., Ferguson, J., Glascock, M., 2012. Chemical Fingerprinting of Kenyan Obsidian Sources and Late Quaternary Artifacts With Electron Microprobe Presented at the Annual Meeting of the Society for American Archaeology, Memphis, Tennessee.
- Speakman, R.J., Shackley, M.S., 2013. Commentary: silo science and portable XRF in archaeology: a response to Frahm. J. Archaeol. Sci. 40, 1435–1443.
- Stojanowski, C.M., Carver, C.L., Miller, K.A., 2014. Incisor avulsion, social identity and Saharan population history: new data from the Early Holocene southern Sahara. J. Anthropol. Archaeol. 35, 79–91.
- Torrence, R., White, P., Kelloway, S., 2012. Expanding the range of PXRF to ethnographic collections. IAOS Bull. 46, 9–14.
- Turton, D., 1986. A problem of domination at the periphery: the Kwegu and the Mursi. The Southern Marches of Imperial Ethiopia: Essays in History and Social Anthropology 33. Cambridge University Press, Cambridge, p. 148.
- Tykot, R.H., Lai, L., Tozzi, C., 2011. In: Turbanti-Memmi, I. (Ed.), Intra-site obsidian subsource patterns at Contraguda, Sardinia (Italy). Proceedings of the 37th International Symposium on Archaeometry. Springer, pp. 321–328.
- Tykot, R.H., Freund, K.P., Vianello, A., 2013. Source analysis of prehistoric obsidian artifacts in Sicily (Italy) using pXRF. In: Armitage, R.A., Burton, J.H. (Eds.), Archaeological Chemistry VIII, pp. 195–210.
- Vázquez, C., Palacios, O., Parra Lue-Meru, M., Custo, G., Ortiz, M., Murillo, M., 2012. Provenance study of obsidian samples by using portable and conventional X-ray fluorescence spectrometers. Performance comparison of both instrumentations. J. Radioanal. Nucl. Chem. 292, 367–373.
- Williams, P.R., Dussubieux, L., Nash, D., 2012. Chapter 6: provenance of Peruvian Wari obsidian: comparing INAA, LA-ICP-MS, and portable XRF. In: Liritzis, I., Stevenson, C.M. (Eds.), Obsidian and Ancient Manufactured Glasses. University of New Mexico Press, pp. 75-85.
- Williams-Thorpe, O., 2008. The application of portable X-ray fluorescence analysis to archaeological lithic provenancing. In: Potts, P.J., West, M. (Eds.), Portable X-ray Fluorescence Spectrometry: Capabilities for In Situ Analysis. The Royal Society of Chemistry, Cambridge, pp. 174–205.
- Wilshaw, A., 2016. The current status of the Kenya Capsian. Afr. Archaeol. Rev. 33, 13–27.
  Wilson, L., Pollard, A.M., 2001. The provenance hypothesis. In: Brothwell, D.R., Pollard, A.M. (Eds.), Handbook of Archaeological Sciences. John Wiley and Sons, Chichester, pp. 507–517.